RICE UNIVERSITY

Analysis of Hysteretic Systems: Preisach Formalism and Bouc-Wen Modeling
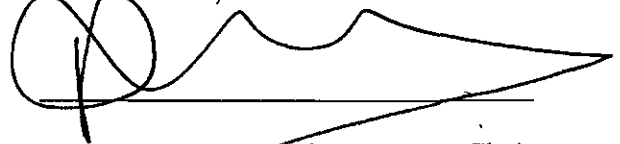
By

Michael Grimmer

A THESIS SUBMITTED IN PARTIAL FULFILLMENT OF THE REQUIREMENTS FOR

THE DEGREE

Master of Science

APPROVED, THESIS COMMITTEE:

Pol D. Spanos, Chair
Lewis B. Ryon Professor of Mechanical Engineering

Fathi H. Ghorbel
Professor of Mechanical Engineering

Leonardo Dueñas-Osorio
Associate Professor of Civil and Environmental Engineering

HOUSTON, TEXAS
APRIL 2017

ABSTRACT

Analysis of Hysteretic Systems: Preisach Formalism and Bouc-Wen Modeling

By

Michael Grimmer

The inherently nonlinear phenomenon of hysteresis is notoriously difficult to model. Of notable interest are the inverse models of hysteresis which identify the parameters of a particular model to closely match experimental data. Two major models of hysteresis are the Preisach and Bouc-Wen models. As researchers typically deal with solely one model for their analyses, this thesis initially develops techniques to convert from the Bouc-Wen model to the Preisach model, using first a least squares fit followed by using artificial neural networks. The parameters of each of the two models are investigated in further detail, with emphasis on how each parameter affects the loop and how to arrive at an adequate initial estimate for the identification problem algorithms. The techniques are then evaluated and compared against several sets of experimental data for hysteresis loops supplied by the Air Force Research Lab. Their optimized solutions are compared to assess the flexibility and viability of each model. Generally, it is found that, while both models are successful, the Preisach model is more flexible in fitting different types of experimental loops. Lastly, both experimental loops and theoretical loops subjected to white noise are identified using Transitional Markov Chain Monte Carlo (TMCMC) algorithms via the Preisach model. These results show promise for the TMCMC method being applied on data, particularly when the loop is induced by white noise.

Acknowledgments

First and foremost, I would like to extend my thanks to Dr. Pol Spanos. His unbounded optimism and enthusiasm has been very encouraging during my research. Further, his intimate knowledge of hysteresis, Monte Carlo, and stochastic mechanics has been supremely appreciated.

I would also like to thank Dr. Fathi Ghorbel and Dr. Leonardo Dueñas-Osorio for serving on my thesis committee. Their edits and commentary are very much welcomed and appreciated.

I thank both Rice University and the United States Air Force for funding this master's degree. Without the scholarship from Rice University and the financial support from the Air Force, this venture would not have been possible. Dr. Abdellah Lisfi's group at Morgan State University has also been helpful in supplying hysteresis data from the Air Force Research Lab.

Immense thanks also goes to Giovanni Malara, who is currently serving as a postdoctoral fellow of marine engineering at the Natural Ocean Engineering Laboratory at the University of Reggio Calabria. He has been a great help these past two years, and without his aid both conceptually and in coding, I would likely have not been able to achieve the goals of this thesis as much as I have.

Lastly, I would like to thank my friends and family for their stalwart and undying support. Their encouragement has always inspired me to reach for my highest goals.

Table of Contents

Chapter 3: On the Conversion of Bouc-Wen Parameters to Preisach Parameters   26

Chapter 4: Revisiting Preisach and Bouc-Wen Parameter Effects   41

Chapter 5: Performance of Preisach Parameters and Bouc-Wen Parameters on Experimental Data   54

Chapter 6: System Identification of Hysteresis Loops Using Transitional Markov Chain Monte Carlo Based Bayesian Approach   60

Chapter 7: Concluding Remarks   79

List of References   83

List of Figures

List of Tables

<u>Chapter 1</u>

Introduction

1.1   The Phenomenon of Hysteresis

Hysteresis is a widely observed phenomenon, both in nature and in constructed systems. It manifests itself in many fields, including fundamental physical mechanisms [1] and as the consequence of degradation and imperfections in mechanical systems. Further, it can be purposefully built into a system to monitor behavior [2]. One of the first mentions of hysteresis was in a paper published by Ewing, where he noticed that a lagging effect of the thermoelectric quality of stretched wire with respect to the associated tensile stress on the wire [3]. He also observed that the effect was static; that is, the "lagging" effect was unaffected by the rate at which the load was changed. He observed a similar phenomenon with his magnetic materials. Thus, Ewing named this effect hysteresis, which stems from Greek, meaning "to lag behind." In his studies, Ewing highlighted two of the critical features of hysteresis: lagging and rate-independence.

The lagging effect can be effectively described by the notion that a system experiencing hysteresis contains a retardation of an effect when the forces acting upon the body are changed. The second property, rate independence, means that an input-output plot depends on the value of the input, but not the speed at which the input is changed [4].

Research on hysteresis related phenomena continued in earnest after Ewing's initial discovery. Some major contributors during this time included Lord Rayleigh, Duhem, and Preisach [5, 6, and 7]. Many models for this nonlinear process were promulgated by the likes of von Mises, Prandtl, Ishlinskii, Hill, and Prager [8, 9, 10, 11, and 12].

While the general nature of hysteresis was known at this time, it remained surprisingly unstudied from a mathematical point of view until the mid-1960s with Bouc, who successfully modeled different hysteretic phenomena [13]. For one of the major kinds of models, the Russian mathematicians Krasnoselskii and Pokrovskii were seminal in giving a more structured formulation to hysteresis by using the concept of operators [14]. This setup was necessary for Mayergoyz to formulate the well-known and widely used Classical Preisach Model [15]. The Preisach model has proven an incredibly versatile tool in hysteresis, and its mathematical foundations will be extensively covered in *Chapter 2*.

Concurrently, the mathematical modeling work completed by Bouc was compounded and generalized by contributions from Wen to form the Bouc-Wen model in 1976 [16]. This model opts for using first-order non-linear differential equations that relate input displacement to output restoring force in a hysteretic manner. This will also be covered in more detail in *Chapter 3*.

1.2   Definition and Visualization of Hysteresis

For the purposes of this thesis, scalar hysteresis is assumed for clarity. Using control theory terminology, consider the simple system of the plant in Figure 1.1 characterized by an input $u(t)$

and an output $f(t)$. The plant can be called a hysteresis transducer if its input-output is a multi-branch non-linearity for which branch-to-branch transitions occur after input extrema [15].

Figure 1.1: General representation of a system

A visual example of the rate-independent property of hysteresis is shown in Figure 1.2. The branches of hysteretic non-linearities are determined by the past extremum values of input, while the speed or path of the input variations between these extremum points has no bearing on the restoring force branching.
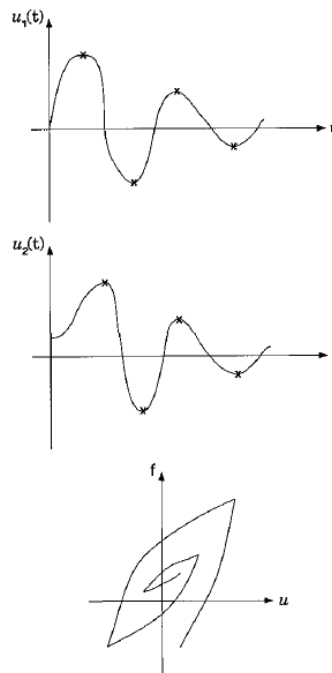
Figure 1.2: Demonstration of rate-independence of hysteresis: (top) Sample input over time, (middle) Different sample input over time, and (bottom) hysteretic restoring force from both inputs

This figure shows that the restoring force of a hysteretic system will remain consistent regardless of the path or speed between extremum points of the input (provided the extremum points are of the same magnitude).

The kind of hysteresis investigated in this thesis is of the form of Figure 1.3. In this common subset of hysteresis, the material experiences a loading and unloading phase. As Figure 1.3 shows, the material will start from negative saturation u_1 and follow the path ABC on the loading phase towards u_2. On the unloading phase, the material will follow the path CDA back towards u_1.
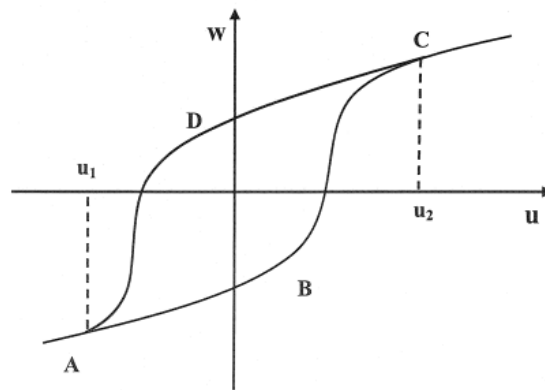
Figure 1.3: Continuous hysteresis loop

A simple analog with a mechanical system is that of a beam pinned at one end. A compressive force is applied to bend the beam downward. Then, the force is lessened, and the decreased force would then cause the end of the beam to return to its original state. However, it would not follow the same path on the stress-strain curve on the unloading and heading for negative saturation as it would for the loading and the heading towards positive saturation. In applying this towards

Figure 1.4, the loading curve would be represented from the first line from quiescent conditions to the positive saturation point.
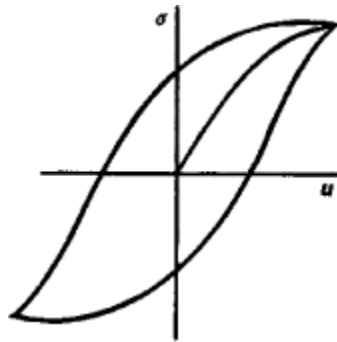
Figure 1.4: Continuous hysteresis loop starting from quiescent conditions

In most of these hysteretic materials, starting either from negative saturation or quiescent conditions, the path of the restoring force will be counter-clockwise. The existing literature on hysteresis generally concerns continuous hysteresis which involves the loops shown in Figure 1.3 and Figure 1.4. Note that hysteresis does not always occur in a closed loop. Hence, a loop is a particular kind of hysteresis that does occur quite often, but is not the only possibility. Some materials can dissipate more energy with each successive loading and unloading cycle, leading to the results in Figure 1.5.
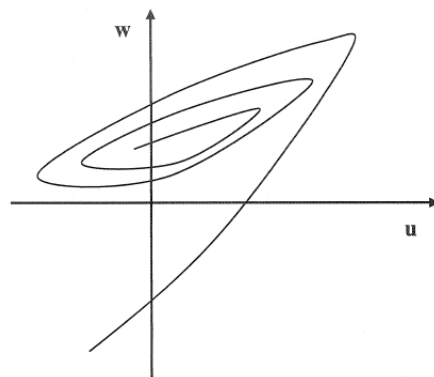
Figure 1.5: Nonlinear hysteretic behavior that does not form a continuous loop

Although hysteresis can be associated with the characteristics of Figure 1.5, this thesis will deal exclusively with hysteresis loops that form a closed loop. With this groundwork, a general definition of hysteresis can be applied. *Hysteresis is the rate independent memory effect, where the term memory expresses the lagging of an effect behind its cause. Whenever and wherever the system exhibits a lag compared to the system's input, then hysteresis is present* [17].

1.3   Models of Hysteresis

Hysteresis models can generally be divided into two classes [17]. This can be shown in Figure 1.6.
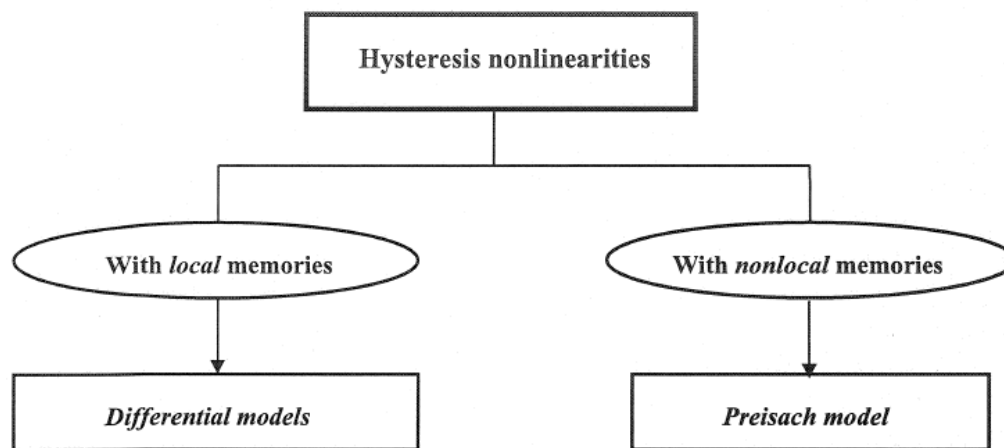
Figure 1.6: Types of hysteresis and their corresponding models of choice

Hysteresis with local memories can be distinguished from other models by one fundamental property. Essentially, the past does not exert any influence on the present or future of the hysteretic system. The standard way of modeling these types of hysteresis loops is via differential models of hysteresis. The primary model that will be used throughout this thesis for local memories is the Bouc-Wen model. One of the advantages of these types of models is that

they may be incorporated directly in the differential equations that govern the motion of particular systems while assigning values to the many parameters that define the system. There are no hysteretic operators in this perspective. Thus, the Bouc-Wen model can often be simpler to model compared to the Preisach model for its reliance on first-order differential equations.

Notably, hysteresis with non-local memories does have the memory effect. Future values depend not only on the present state, but on the history of the input as well. Modeling hysteresis with non-local memories is the theoretical basis of the Classical Preisach Model [15]. Mayergoyz incorporated the idea of simple operators, called hysterons. The resulting product of the Preisach model is one of the most widely used model in literature for its versatility and wide applicability.

Because of these differences in the modeling process, most researchers choose a model for the duration of their work without comparing resulting models across multiple schemes. It is the opinion of this author that, in the operator based models, the Preisach model is more versatile than the traditional Bouc-Wen model in identifying experimental loops, and that for other reasons enumerated later in this thesis, it should in many cases be the preferred model. Note that this thesis deals exclusively with the operator-based Preisach and Bouc-Wen models of hysteresis and not with bilinear models. One of the objectives of this thesis is the comparison on the performance of matching experimental data with both the Preisach and Bouc-Wen models. Further, little to no research has been done on how to convert between these two schemes, should a need arise. As such, another aim of this thesis is to develop ways to convert one system of modeling to the other. Working in the Preisach domain has many advantages over the Bouc-Wen model, to include stochastic averaging and equivalent linearization. Lastly, there has been no

work applying the Transitional Markov Chain Monte Carlo method through the Preisach model on experimental data, particularly data which is exposed to white noise. Bayesian model updating has use because it does not find a single plausible model but a set of models whose predictions are weighted by the probabilities of these models conditioned on the measured data. Due to their ability to consider a set of models, they are suitable for modeling uncertainties in modeling [68].

1.4   Thesis Organization

Chapter 1 deals with an introduction of hysteresis and the popular models associated with it, specifically the Preisach model and the Bouc-Wen model. It also covers the history of the field of hysteresis and the need for the effective modeling of this nonlinear phenomenon.

Chapter 2 deals with the necessary mathematical background for the material to come in later chapters. It covers the theory behind both the Preisach model and the Bouc-Wen model. Furthermore, *Chapter 2* covers the theory behind the artificial neural network, which will be employed (and compared against least squares) in the conversion of Bouc-Wen parameters to Preisach parameters. Neural networks can prove beneficial because of their speed and ease of use, as well as for understanding the complex relationship between the two models. Finally, this chapter covers the theory behind the Monte Carlo method and its possible application towards the inverse modeling of hysteretic systems.

Chapter 3 discusses the conversion of Bouc-Wen parameters into Preisach parameters and the possible benefits of doing so. Both the method of least squares and a built artificial neural

network will be considered. The conversion of Preisach parameters into Bouc-Wen parameters is addressed as well.

Chapter 4 is a study into how model parameters affect the overall shape and size of the hysteresis loop. Relatively little research has been done on this subject (notably when considering the minor variations in the exact kind of models researchers use), and understanding how parameters affect the loop is critical if one hopes to effectively and accurately capture the model from experimental data.

Chapter 5 deals with the application of both models on experimental data provided by the Air Force Research Lab (AFRL). It also invokes an assessment of the performance of these two models on the same set of data and of the advantages of having the models' parameter information when dealing with such materials.

Chapter 6 deals with the Transitional Markov Chain Monte Carlo method and its applicability towards the inverse modeling of hysteresis using the Preisach model. This study deals more with the random and noisy processes of many materials and the search for the posterior probability distribution functions for the parameters of the Preisach model among noisier systems.

Finally, *Chapter 7* is a summary of the entirety of the thesis, delineating what has been accomplished and making suggestions for future work.

Chapter 2

Mathematical Background

2.1   Preliminary Remarks

To establish the scope of this work, attention is first given to the mathematical background and the theory used in building these models and simulations. There are sections devoted separately to the Preisach model and Bouc-Wen model, as well as the theory regarding artificial neural networks and Monte Carlo simulation. With a solid understanding of these concepts, the reader can appreciate work accomplished in later chapters.

2.2   The Preisach Model

2.2.1   Hysterons and Superposition

This section focuses on the formulation of the Preisach model. If the reader wishes to consult further resources on this topic, there are many available resources including the work on the nature of operators by Krasnoselskii and Pokrovskii as well as the backbone of the entire model: Mayergoyz's *Mathematical Models of Hysteresis and their Applications* which formally introduces the concept of the Classical Preisach model [14, 15].

To understand the Preisach model, first consider an infinite set of hysteresis operators $\gamma_{\alpha\beta}$. These operators can take on two values: -1 or 1. Each operator can be visualized with Figure 2.1 as a rectangular loop with the threshold values of α and β. These relays can also be thought to have

an "up" position and a "down" position corresponding with $\gamma_{\alpha\beta} = 1$ and $\gamma_{\alpha\beta} = -1$, respectively. Further, for consistency, the reader can assume that $\alpha \geq \beta$, as supported by Figure 2.1. Note that the hysteron's value can be summarized via Eq. (2.1).

$$\gamma_{\alpha\beta} = \begin{cases} +1 \ if \ u > \alpha \ or \ u > \beta \ and \ decreasing. \\ -1 \ if \ u < \beta \ or \ u < \alpha \ and \ increasing. \end{cases} \tag{2.1}$$
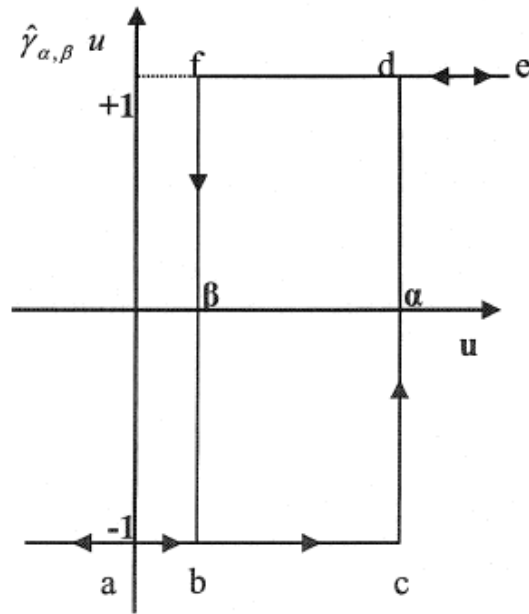
Figure 2.1: A typical hysteron

As the input $u(t)$ is monotonically increased, the ascending branch $abcde$ is followed. As the input $u(t)$ is monotonically decreased, the descending branch $edfba$ is followed. Next, adopt the notion that all hysterons have the same input $u(t)$ and contribute to the same output $f(t)$ in conjunction with a weighting function $\mu(\alpha, \beta)$, which is often called the Preisach function. Then, the Preisach function can be written.

$$f(t) = \hat{\Gamma}u(t) = \iint_{\alpha \geq \beta} \mu(\alpha, \beta)\gamma_{\alpha\beta}u(t)d\alpha d\beta. \qquad (2.2)$$

Here, $\hat{\Gamma}$ denotes the hysteresis operator that is defined by the integral in Eq. (2.2). Thus, the output of the hysteretic system is, in the Preisach model, the weighted sum of the outputs of each hysteron. This is visually represented in Figure 2.2.
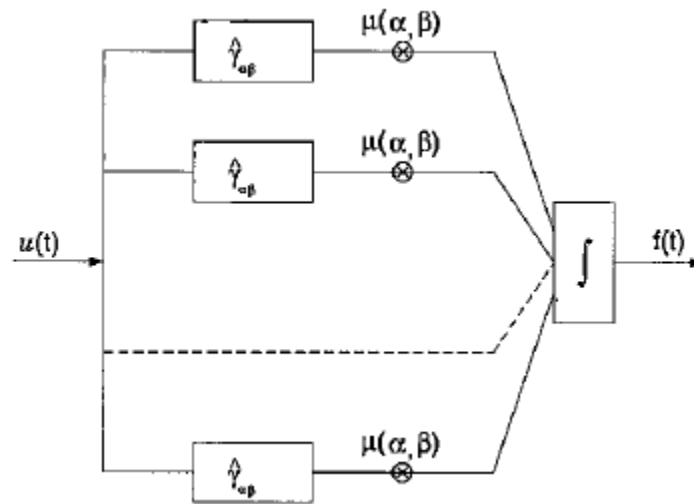
Figure 2.2: Block diagram of the Preisach model; hysterons multiplied by the weighting function

2.2.2 Graphical Representation and the $\alpha - \beta$ Half-Plane

Preisach developed an efficient way of showing the Preisach model's hysterons during simulation. He proposed a half-plane of the α and β values that the Preisach model can have. It is a half-plane limited by a triangle because of the requirement that $\alpha \geq \beta$, and it is shown in Figure 2.3.
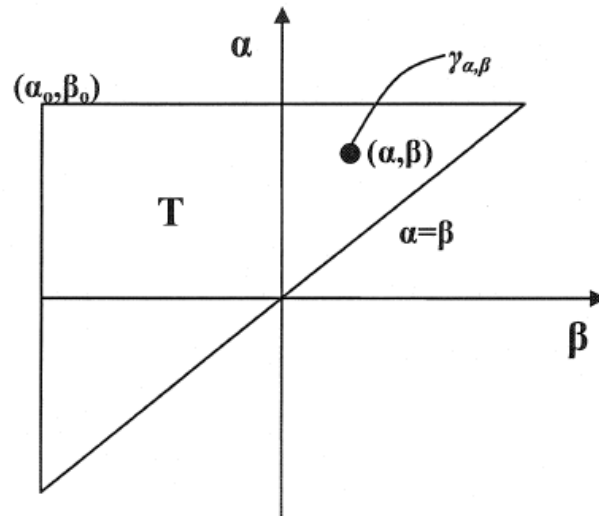
Figure 2.3: The Preisach half-plane within the bounds in the triangle T

The hypotenuse in Figure 2.3 is part of the line $\alpha = \beta$, the limiting case. The vertex of its right angle has the coordinates (α_0, β_0), with $\beta_0 = -\alpha_0$. It can also be assumed that the function is finite. That is, when $\mu(\alpha, \beta)$ is outside of the triangle, its value is zero. It is important to note that in this geometric interpretation it is assumed that the major loop of the hysteretic system is closed. This is a widely held assumption in the literature due to its wide occurrence in materials and will not limit the scope of the Preisach half plane to a significant degree.

To appreciate how the Preisach half-plane affects the loop itself, consider a system starting at negative saturation. This is when all the hysterons have a value of -1 (in the third quadrant of the half-plane shown in Figure 2.3). As the hysterons "switch" from -1 to 1, the graphical analogy shows that the subdivision of $\alpha = u(t)$ moves upward. This happens with monotonic increasing input until the positive saturation point (the top side of the triangle in Figure 2.3) is reached. As the material experiences the unloading phase, it travels along the different path

$edfba$ from Figure 2.1. In the Preisach half-plane from Figure 2.3, this is represented by the moving line $\beta = u(t)$ from right to left. With the part of the half-plane that has hysterons with the value of 1, that part of the graph is subdivided with the notation $S^+(t)$. Likewise, the half-plane section with hysterons in the "off" position of -1 is subdivided with the notation $S^-(t)$. If the material monotonically increases again, (but not until positive saturation), then the hysterons will turn "on" with the instantaneous $u(t)$. These "links" in the $S^+(t)$ and $S^-(t)$ domains will then form a staircase pattern in Figure 2.5, as shown with the following sample time history in Figure 2.4.
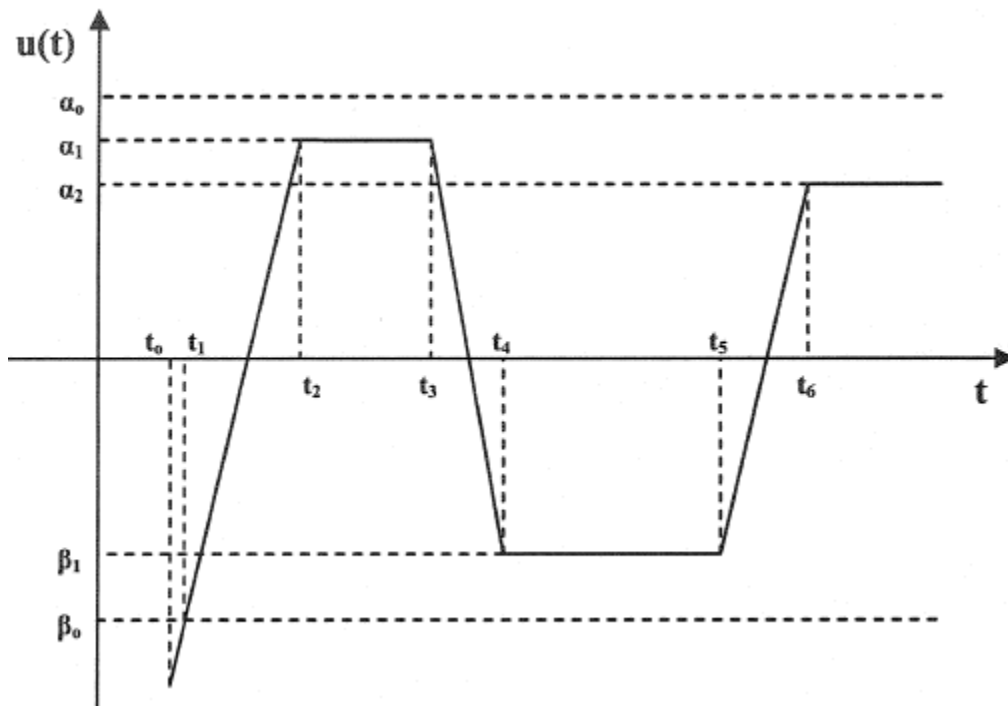
Figure 2.4: Sample time history of input
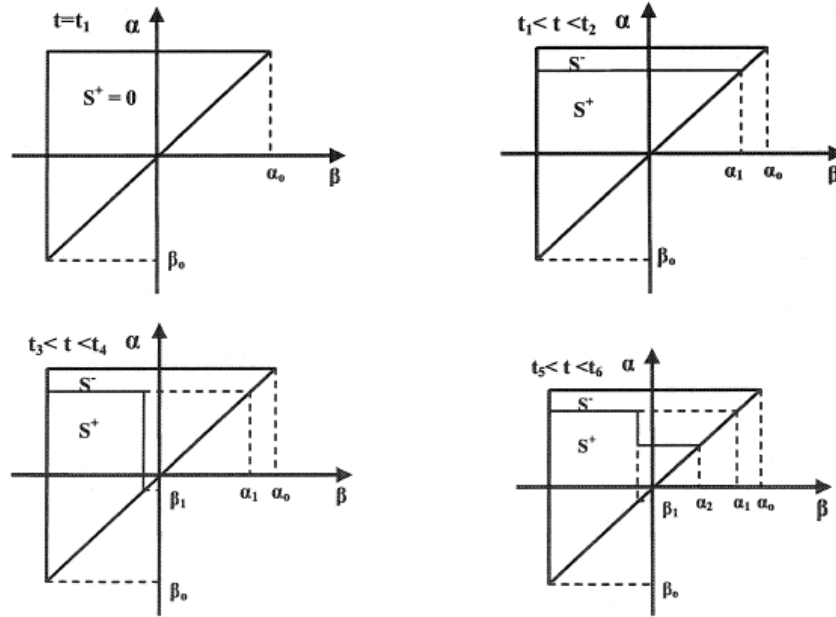
Figure 2.5: Sample time history on Preisach half-plane; at t_1 (top left), at $t_1 < t < t_2$ (top right), at $t_3 < t < t_4$ (bottom left), and at $t_5 < t < t_6$ (bottom right)

This input history can be succinctly summarized via Figure 2.6, which shows the evolution of the interface $L(t)$ with the aforementioned time history.
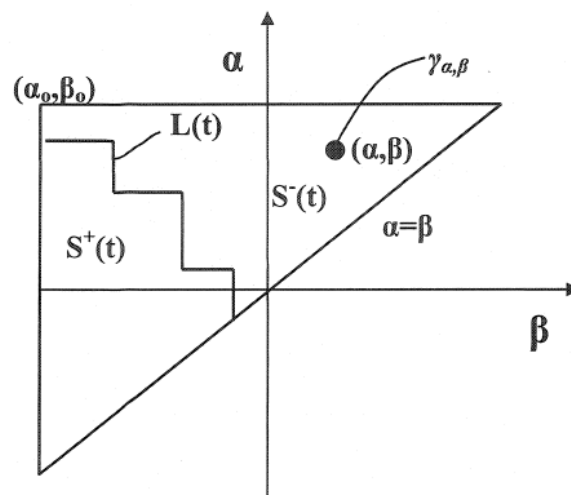
Figure 2.6: Evolution of interface $L(t)$ with sample time history

This visualization can be compared side-by-side with the input $u(t)$ against the output $f(t)$ to

see how one directly affects the other. This is accomplished in Figure 2.7 and Figure 2.8.
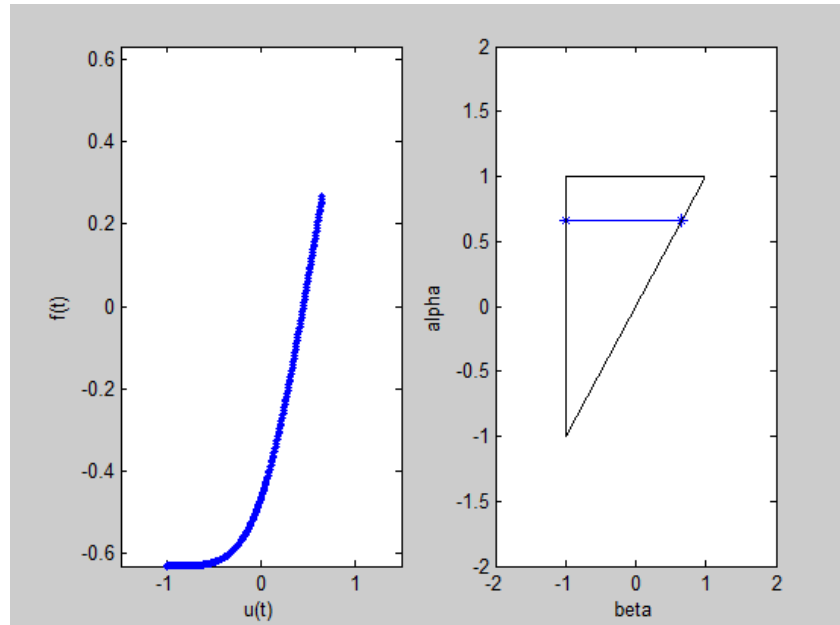
Figure 2.7: Hysteresis curve $u(t)\, vs.\, f(t)$ and $\alpha - \beta$ half-plane on loading phase
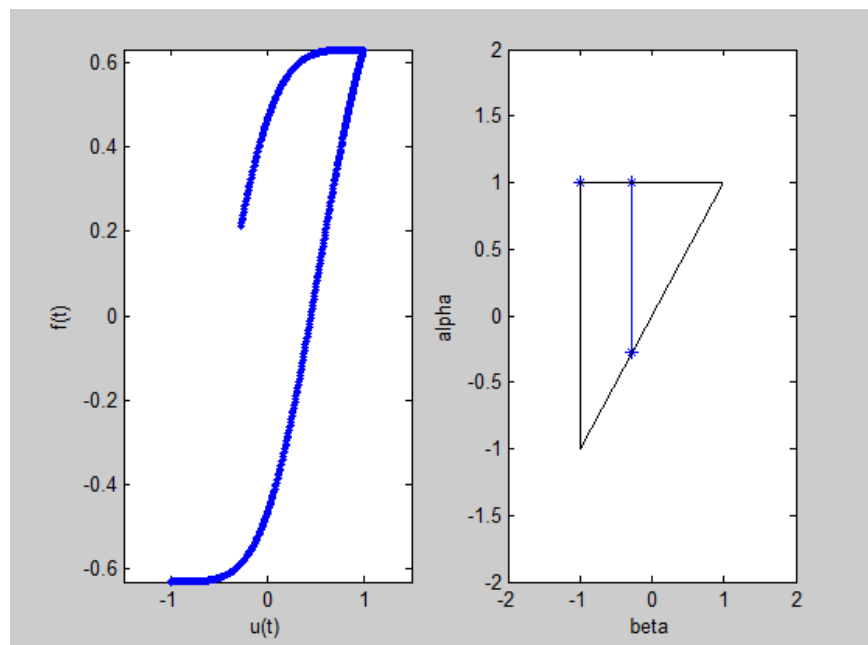
Figure 2.8: Hysteresis curve $u(t)\, vs.\, f(t)$ and $\alpha - \beta$ half-plane on unloading phase

2.2.3 Identification Problem

The crux of the identification problem of Preisach curves stems from the identification problem of $\mu(\alpha, \beta)$. Mayergoyz describes a possible solution using first-order reversal curves [15]. He proposes to consider a system in the state of negative saturation. Then, the material is subjected to a monotonic increase in loading until it reaches the value of α'. The corresponding value for the output is $f_{\alpha'}$. A first-order transition curve is formed with the subsequent monotonic decrease to some value β'. The output at this point is $f_{\alpha'\beta'}$.
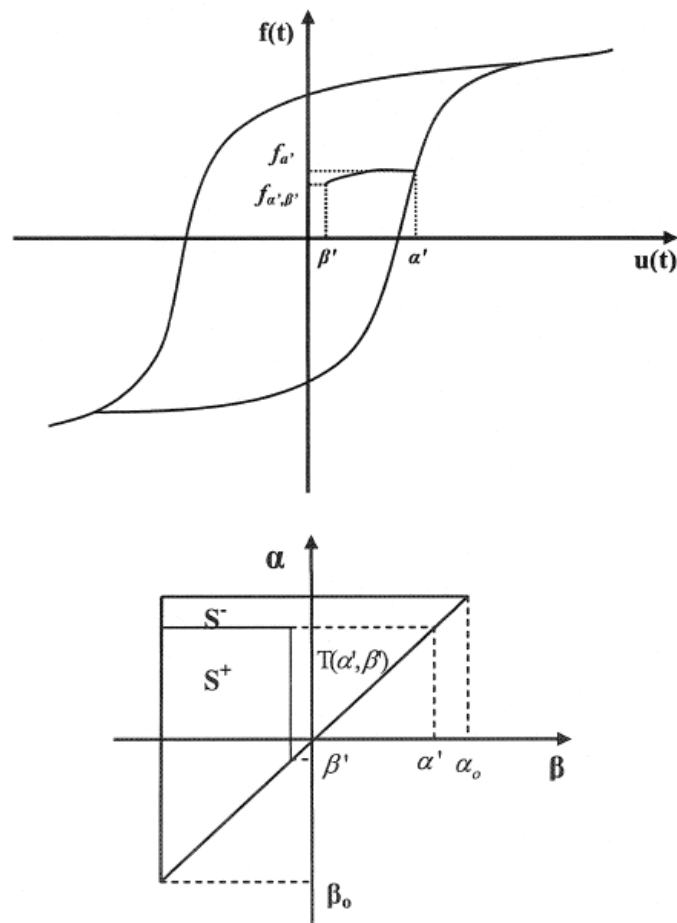
Figure 2.9: First-order reversal hysteresis curve (top) and respective Preisach half-plane (bottom)

The function in Eq. (2.3) can be defined.

$$F(\alpha',\beta') = \frac{1}{2}(f_{\alpha'} - f_{\alpha'\beta'}). \tag{2.3}$$

Based off of Eq. (2.2) and Eq. (2.3), Eq. (2.4) can be obtained.

$$f_{\alpha'\beta'} - f_{\alpha'} = -2\iint_{\Gamma(\alpha',\beta')} \mu(\alpha,\beta)\gamma_{\alpha\beta}u(t)d\alpha d\beta = F(\alpha',\beta') \tag{2.4}$$

$$= \iint_{\Gamma(\alpha',\beta')} \mu(\alpha,\beta)\gamma_{\alpha\beta}u(t)d\alpha d\beta.$$

After differentiating twice with respect to α and β, the following result is produced.

$$\mu(\alpha',\beta') = -\frac{\partial^2 F(\alpha',\beta')}{\partial\alpha'\partial\beta'} = \frac{1}{2}\frac{\partial^2 f_{\alpha'\beta'}}{\partial\alpha'\partial\beta'}. \tag{2.5}$$

The first-order reversal curve method works well in theory. However, partially because of the double numerical differentiation, it is prone to inaccuracies. Therefore, an alternative approach is adopted herein from the work done by Spanos, Ktena, Massalas, and Fotiadis [18, 19]. It assumes a bivariate Gaussian distribution of the weighting function, such as

$$\mu(\alpha,\beta) = \frac{1}{2\pi\sigma_\alpha\sigma_\beta\sqrt{1-\rho^2}}\exp\left\{-\frac{1}{2(1-\rho^2)}\left[\left(\frac{\alpha-\mu_\alpha}{\sigma_\alpha}\right)^2\right.\right. \tag{2.6}$$

$$\left.\left.- 2\rho\left(\frac{\alpha-\mu_\alpha}{\sigma_\alpha}\right)\left(\frac{\beta-\mu_\beta}{\sigma_\beta}\right) + \left(\frac{\beta-\mu_\beta}{\sigma_\beta}\right)^2\right]\right\}.$$

In Eq. (2.6), the parameters to be determined are $\mu_\alpha, \mu_\beta, \sigma_\alpha, \sigma_\beta$, and ρ. They stand for the ascending mean, descending mean, ascending standard deviation, descending standard deviation, and correlation coefficient, respectively. In other literature proposed by Spanos et al., they

proposed symmetric parameters [21-23]. That is, $\mu_\alpha = \mu_\beta, \sigma_\alpha = \sigma_\beta$ and $\rho = 0$. This yields Eq. (2.7).

$$\mu(\alpha, \beta) = \frac{1}{2\pi\sigma^2} \exp\left\{-\frac{1}{2}\left[\left(\frac{\alpha - \mu}{\sigma}\right)^2 + \left(\frac{\beta - \mu}{\sigma}\right)^2\right]\right\}. \tag{2.7}$$

This can be applied in many cases where the loop is symmetric for simplicity's sake.

2.3   The Bouc-Wen Model

As stated in *Chapter 1*, the Bouc-Wen model deals with first-order differential equations. It requires seven parameters to describe the hysteresis phenomenon. The effect of the parameters on the shape of the hysteresis loop is highly nonlinear and difficult to assess [24], but helpful relationships will be established in *Chapter 4*. For these reasons, it has been used comparatively less in the field of magnetism [25] and more in engineering mechanics. The Bouc-Wen model has been promoted for its application to inverse problems – that is, where a set of experimental data points is given and it is required to evaluate the model parameters that will produce a curve which follows the experimental data with the least error [16, 26]. However, in ensuing chapters, it will be shown that it is ideal to model certain types of hysteresis loops, but there are other loop shapes where it is less optimal.

Consider the equation of a single degree of freedom system

$$m\ddot{x}(t) + c\dot{x}(t) + F(t) = u(t). \tag{2.8}$$

In Eq. (2.8), m is the mass, $x(t)$ is the displacement, c is the linear viscous damping coefficient, $F(t)$ is the restoring force, and $u(t)$ is the excitation force. According to the relationships defined in the literature of Bouc and Wen, the following relationship can be defined.

$$F = a\frac{F_y}{u_y}u + (1-a)F_y z. \tag{2.9}$$

In Eq. (2.9), $a = \frac{k_f}{k_i}$ is the ratio of post-yield to pre-yield (elastic) stiffness, $k_i = \frac{F_y}{u_y}$ is elastic stiffness, F_y is the yield force, u_y is the yield displacement, and $z(t)$ is non-observable dimensionless hysteretic parameter that obeys a single non-linear differential equation with zero initial condition described below.

From this, the Bouc-Wen model can be described a system of nonlinear differential equations governed by the equations [25, 27]

$$\begin{cases} \ddot{x} + 2\zeta\omega_n\dot{x} + \alpha\omega_n^2 x + (1-\alpha)\omega_n^2 z = u(t) \\ \dot{z} = -\gamma|\dot{x}||z|^{n-1}z - \beta\dot{x}|z|^n + A\dot{x} \end{cases}. \tag{2.10}$$

The second part of Eq. (2.10) can be recast as

$$\dot{z}(t) = \dot{u}(t)\{A - [\beta sign(z(t)\dot{u}(t)) + \gamma]|z(t)|^n\}. \tag{2.11}$$

where the symbol $sign$ denotes the signum function.

In these equations, $u(t)$ is a normalized forcing function, and there are seven parameters. These are: the rigidity ratio α ($0 \leq \alpha \leq 1$), the linear elastic damping ratio ζ ($0 \leq \zeta \leq 1$), the pseudo-natural frequency of the system ω_n, the hysteresis controlling amplitude A, and the hysteresis loop shape controlling parameters β, γ, and n. By varying these seven parameters, a wide range of hysteresis loops can be described.

The variable z is a fictitious displacement related to the actual displacement, x [27]. Plotting z against x yields the familiar hysteresis loop. From Eq. (2.10), state space representations have proved fruitful in solving the Bouc-Wen model [25, 28]. The state space representation of Eq. (2.10) can be put in the form

$$\begin{cases} \dot{Y}_1 = Y_2 \\ \dot{Y}_2 = -2\zeta\omega_n Y_2 - \alpha\omega_n^2 Y_1 - (1-\alpha)\omega_n^2 Y_3 + u(t). \\ \dot{Y}_3 = -\gamma|Y_2||Y_3|^{n-1}Y_3 - \beta Y_2|Y_3|^n + AY_2 \end{cases} \tag{2.12}$$

These three differential equations can be simultaneously solved for the hysteresis loop when translated to $[Y_1\ Y_2\ Y_3]^T = [x\ \dot{x}\ z]^T$ [29].

2.4   Artificial Neural Networks

The employment of artificial neural networks (ANNs) can be beneficial towards hard-to-solve nonlinear problems, such the ones involved in modeling hysteresis. The ANN is a computing system made up of a number of simple, highly interconnected processing elements, neurons, which process information in parallel in response to external inputs [30]. Further, it has powerful fault tolerant computing ability which has been used to model a wide range of systems for which mathematical models either cannot be defined or are ill-defined. For this reason, ANNs are a

viable tool for an objective of this thesis that is highly nonlinear in nature: the conversion of Bouc-Wen parameters to Preisach parameters. Because of the fundamentally different nature of these models (one being based in the aggregation of hysterons and one being based in differential equations), there are no equations or procedures that adequately describe the transformation from one domain to the other. In theory, ANNs can approximate an arbitrary nonlinear function with high precision [31-33].

ANNs traditionally work by having an input layer, a hidden layer, and an output layer. This is shown in Figure 2.10. Given enough "training" of the network, the hidden layer weights are updated in the learning process via multiplication and addition biases to convert the input layer to the output layer.
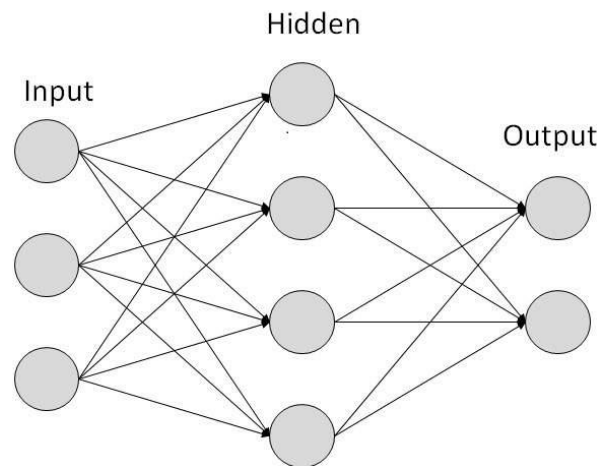
Figure 2.10: ANN architecture

The ANN consists of an input vector. In the cases of hysteresis, this is usually done with the ordinate vector for the hysteresis loop. A training set of input vectors, traditionally on the order of $500 - 1000$ ordinate vectors, is used to train the ANN [34]. This is then converted using the

hidden layer of weights and biases into the output layer, which is traditionally a vector of the parameters. After the ANN is sufficiently trained, it can be applied towards an experimental loop. With the input of the ordinate vector, the ANN will almost immediately output the parameters that create that loop.

This ANN architecture has been applied in the literature towards both the Preisach model and Bouc-Wen model individually, and only under relatively limited circumstances [33-37]. However, there has been no work done on converting one model towards another. Converting from the Bouc-Wen model to the Preisach model can prove useful in applications where the user wishes to apply techniques such as equivalent linearization or stochastic averaging with the Preisach model that would be impossible with the Bouc-Wen model.

However, there has been no work done on converting one model towards another, which this thesis will address in *Chapter 3*.

2.5   Monte Carlo Simulation

Often in experiments there is some inherent noise in the signal. In real world applications, there is an inherent level of randomness that cannot be analytically described. This is especially true in the fields of wing vibration due to turbulence, mechanical vibrations in a system, seismic shaking of buildings, etc. Stochastic differential equations involve at least one of the variables being stochastic in nature. An obvious example for the aforementioned processes is white noise. In general, these stochastic differential equations are harder to treat than their deterministic counterparts. Some analytical schemes that exist include statistical linearization, the method of

moment closure, perturbation, and Markov methods [38, 39]. Due to the difficulty of arriving at analytical solutions with nonlinear systems subjected to white noise, alternative solutions have been proposed. One such solution is the Monte Carlo method, which is based on performing numerical simulations via a computer [40-43]. This theory was formulated in the era succeeding World War II, where scientists were solving problems such as neutron diffusion or transport through an isotropic medium. The name is in relation to the well-known European principality of Monte Carlo casinos and deals with the generation of random numbers. In regards to solving stochastic differential equations, Monte Carlo simulation is based on the fundamental observation that these stochastic phenomena can be treated as an infinite set of deterministic equations. In random vibration theory, the Monte Carlo method is normally used to numerically assess the validity of analytical computations [38, 39, and 44].

Monte Carlo analysis involves simulations in which a large number of experiments are conducted to derive statistical properties of the nonlinear system within some confidence interval. Random numbers are generated from some specific distribution. For the purposes of this thesis, they will generally be drawn from the Gaussian distribution. This set is used to form a sample function of the excitation, which is then used as an input to the nonlinear system. By repeating the procedure several hundreds of times, a collection of response functions is created. With this collection, statistical analysis can be performed. An advantage of the Monte Carlo method is that it can be used for both stationary and non-stationary response statistics. Generally speaking, the larger the data set, the better the estimate statistics will be.

Monte Carlo simulation will be incorporated in *Chapter 6*, wherein the probability distribution functions (PDFs) of Preisach models will be examined. Specifically, it will deal with Transitional Markov Chain Monte Carlo Theory (TMCMC) to avoid the problem of sampling from difficult target probability functions. Instead, it will sample from a series of intermediate PDFs that converge towards the target PDF and are therefore easier to sample.

2.6   Summary

With this strong mathematical background, the following chapters can address the analysis and applications of the Preisach model, the Bouc-Wen model, ANNs, and Monte Carlo simulation. The formulation of the Preisach and Bouc-Wen models are essential for their application in later chapters. ANNs are used in *Chapter 3* for their use in converting parameters from one scheme to the other. Monte Carlo simulation will be applied in *Chapter 6* with arriving at Preisach model parameters, given an experimental loop.

Chapter 3

On the Conversion of Bouc-Wen Parameters to

Preisach Parameters

3.1   Preliminary Remarks

In the literature pertaining to the modeling of hysteresis, the authors address the question of which model of hysteresis to be used and adhere to it. There has been some work discussing the feasibility of producing Preisach model parameters by a trained artificial neural network, given the prerequisite that there is already sample data fed into the network to train it. However, no work has been done on the conversion of one set of parameters to the other. The Bouc-Wen model certainly has several areas of application, but, in general, the Preisach model is more versatile in the application of stochastic averaging and the different types of loops that it can fit. Further, analysis can be done to determine the equivalent linearization in the form of equivalent stiffness and damping which could be helpful in understanding a material's behavior. Therefore, it would be beneficial to be able to convert a loop described by the Bouc-Wen model to the same loop described by the Preisach model. One important caveat to this entire body of work is that both the displacement and restoring force are normalized to be within the bounds $[-1,1]$. This is done for simplicity and ease of comparison. The parameters for both models are easily scalable for other cases.

3.2   Methods of Conversion

3.2.1   Method of Least Squares

This is the most straightforward of approaches on the conversion of Bouc-Wen to Preisach parameters. The term "least squares" refers to the notion that the overall solution minimizes the sum of the squares of the errors made in the difference of results. The best fit in the least squares sense minimizes the sum of squared residuals. The least squares method in this study refers to nonlinear least squares because it requires iterative refinement. It is thus dependent on a reasonable starting estimate from which to converge via iteration. The least squares method was created by Gauss and published by Legendre [45-46].

To effectively use the least squares method, a hysteresis loop needs to be generated as a baseline via the Bouc-Wen model. The best way to validate the conversion model is to generate loops with a degree of randomness within certain bounds. The Bouc-Wen model is very dependent on parameter ranges, as there are many combinations of parameters that will lead to unusable results. The parameter ranges given in the papers by Ye and Wang prove to be reasonable bounds for many of the more common hysteresis loops [28, 31, and 47]. These parameter ranges are given in Table 3.1 below. Parameters in this range have proven to be stable and form complete loops.

Parameter	Lower Limit	Upper Limit
α	0.2	0.8
β	3.0	5.0
γ	1.1	3.0
ζ	0.0	0.2
ω_n	2.0	4.0
A	0.4	1.1
n	1.0	2.0

Table 3.1: Sample Bouc-Wen parameter ranges

For certain types of hysteresis loops, these parameter bounds are adequate. However, for loops that have quite large area or are incredibly "skinny" in the vertical direction, then parameter ranges need to be extended. With a sample loop generated with randomized Bouc-Wen parameters comes the task of fitting the correpsonding Preisach loop. An initial concern is the order of the Bouc-Wen vectors. In the generation of a Bouc-Wen loop, the differential equations draw the loop from quiescent conditions. Thus, the first concern of the code is that of restructuring. The Bouc-Wen loop is also prone to have variability in its amplitude before settling in a more consistent pattern after several iterations. Thus, the Bouc-Wen model is allowed to run for many cycles, with the last complete cycle being used as the baseline loop. Further, a complete loop for Bouc-Wen runs from positive saturation in a clockwise fashion, very much dissimilar to the Preisach formalism of starting from negative saturation and counterclockwise. Therefore, the Bouc-Wen vectors are restructured to start from the Preisach equivalent of negative saturation.

The Preisach model parameters are allowed to have a much broader spectrum, as there are fewer bounds that lead to unusable results. This makes the fitting more flexible, provided that there is a reasonble starting estimate for the parameters. The parameter ranges for the Preisach model for this exercise are shown in Table 3.2.

Parameter	Lower Limit	Upper Limit
μ_α, μ_β	$-\infty$	∞
$\sigma_\alpha, \sigma_\beta$	0	∞
ρ	-1	1
k	0	∞

Table 3.2: Sample Preisach parameter ranges

As shown, μ and σ can take on any real value and still yield reasonable results. The correlation coefficient ρ is bounded between the values of -1 and 1. The scaling coefficient k is bounded by positive real numbers.

Below is a sample run of randomized Bouc-Wen values with the fitted Preisach parameters. Figure 3.1 shows the fit itself. Table 3 and Table 4 show the parameters for Bouc-Wen and the fitted parameters for Preisach, respectively. For these loops, the error was determined by root mean square error.
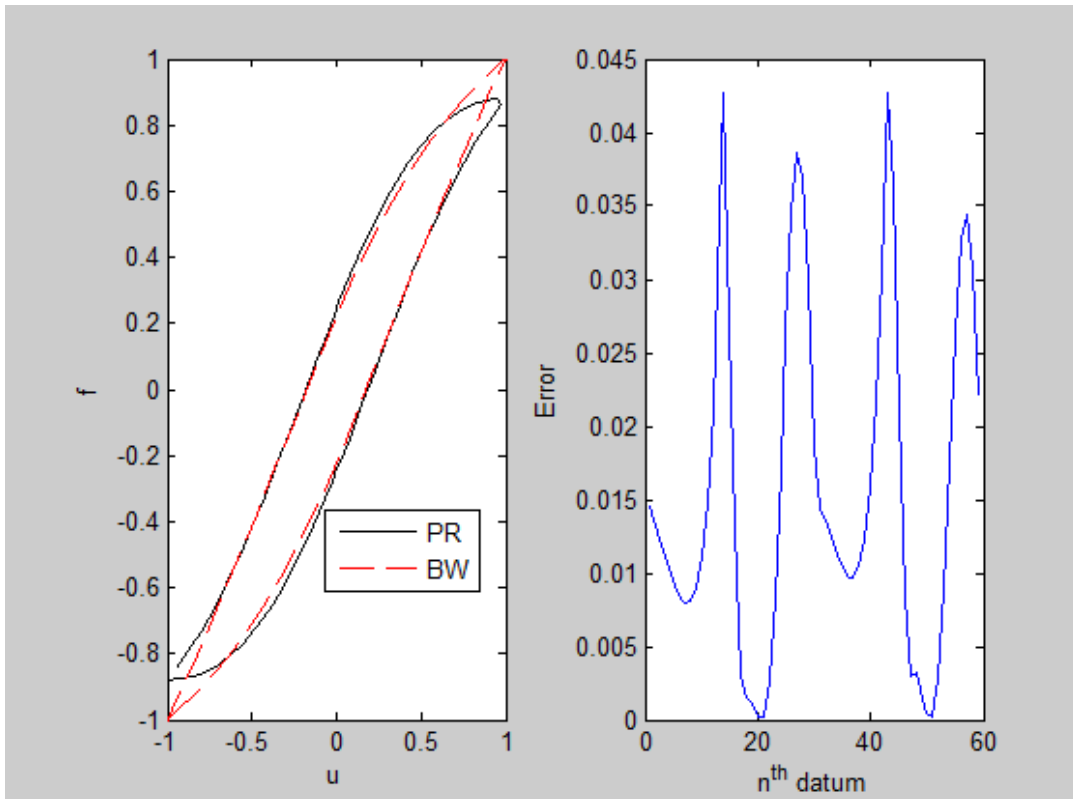
Figure 3.1: Fitted Preisach loop with sample Bouc-Wen loop

Parameter	Value
α	0.2214
β	4.6983
γ	2.8746
ζ	0.1357
ω_n	3.5155
A	0.9202
n	1.3922

Table 3.3: Sample Bouc-Wen values

Parameter	Value
μ_α, μ_β	$0.6346, -0.6184$
$\sigma_\alpha, \sigma_\beta$	$0.7504, 0.7443$
ρ	0.3160
k	14.7748

Table 3.4: Fitted Preisach values

For the fitted Preisach values, it is important to note that, while assuming a symmetric loop is a good starting point, there could be slight variations in the generated Bouc-Wen loop. Having the capability of some asymmetry allows for better least squares minimization by fine-tuning the correlation coefficient.

To develop an adequate set of initial conditions for the Preisach fit, the following procedure is used. Consider the problem of determining the parameters of a bivariate Gaussian distribution for fitting a Preisach model to a given experimental loop. If a least squares approximation is sought, then there must be an appropriate initial estimate leading to an adequate approximation of the experimental hysteresis loop. This problem can be solved by using a geometrical line of reasoning and by exploiting the nature of the Gaussian bivariate distribution. The idea is the following:

For calculating the Preisach force, Eq. (3.1) applies as [15]

$$f(t) = -F(\alpha_0, \beta_0) + 2\sum_{k=1}^{n(t)}[F(M_k, m_{k-1}) - F(M_k, m_k)]$$

(3.1)

Thus, for the ascending and descending curves is specifically recast, respectively, as

$$f^+(t) = -F(\alpha_0, \beta_0) + 2\sum_{k=1}^{n-1}[F(M_k, m_{k-1}) - F(M_k, m_k)] + 2F(u(t), m_{n-1}) \qquad (3.2)$$

and

$$f^-(t) = -F(\alpha_0, \beta_0) + 2\sum_{k=1}^{n}[F(M_k, m_{k-1}) - F(M_k, m_k)] + 2[F(M_n, m_{n-1}) - F(M_k, u(t))]. \qquad (3.3)$$

It is seen that for reproducing a given hysteresis loop one can neglect the influence of the past terms. This is like computing numerically the force by going straight from negative saturation to positive saturation, and then back again to negative saturation. In this manner, one obtains

$$f^+(t) = -F(\alpha_0, \beta_0) + 2F(u(t), \beta_0) \qquad (3.4)$$

and

$$f^-(t) = F(\alpha_0, \beta_0) - 2F(\alpha_0, u(t)). \qquad (3.5)$$

Next, restrict attention to the case in which the distribution function is a bivariate normal with zero correlation coefficient and equal means and standard deviations to arrive at computationally cheaper method for calculating $F(\alpha, \beta)$. In this context, the functions involving the integration of the distribution are explicitly calculated as

$$F(\alpha,\beta) = \frac{1}{8}k\left[erf\left(\frac{\alpha-\mu}{\sigma\sqrt{2}}\right) - erf\left(\frac{\beta-\mu}{\sigma\sqrt{2}}\right)\right]^2. \tag{3.6}$$

This is equation is quite useful because it allows calculating directly the Preisach force without computationally costly calculations and, further, it can be integrated analytically. It is seen that the unknown parameters are μ, σ and k (a constant included for conveniently changing the magnitude of the force at negative saturation). Thus, three conditions must be posed for their determination. For this purpose, three geometric conditions for "reproducing" the general features of the experimental loop must be considered. The conditions are:

1) The center of the experimental loop must be the same of the Preisach loop, f_c.

2) The area into the experimental loop must be the same of the Preisach loop, A.

3) The "vertical distance" between negative and positive saturation must be identical in the Preisach and in the experimental loop, Δf_{max}.

These quantities readily from Eq. (3.4) and Eq. (3.5); the following system of equations is derived

$$\begin{cases} kF\left(\frac{u_s^- + u_s^+}{2}, u_s^+\right) - kF\left(-u_s^-, \frac{u_s^- + u_s^+}{2}\right) = f_c \\ 2kF(-u_s^-, u_s^+)(u_s^- + u_s^+) - 2k\int_{-u_s^-}^{u_s^+}[F(u(t),u_s^+) + F(-u_s^-,u(t))]du(t) = A. \\ 2kF(-u_s^-, u_s^+) = \Delta f_{max} \end{cases} \tag{3.7}$$

where:

- u_s^- and u_s^+ are displacement values (both positive) associated with negative and positive saturation;

- f_c is the ordinate of the center of the experimental loop (note that the abscissa of the center is at $(u_s^+ - u_s^-)/2$;

- A is the area into the experimental loop;

- Δf_{max} is the difference between the maximum and the minimum values of the experimental loop (vertical distance between the extremes of the experimental loop).

The integral in the second equation is kept for simplicity of notation, but it can be explicitly calculated. Eq. (3.7) is a system of nonlinear algebraic equations that can be readily solved. The first iteration is assumed to have the quantities $\mu = 0, \sigma = 1$, and $k = 1$, as these values consistently converge to a good initial estimate.

With this procedure, an adequate initial Preisach estimate can be procured. In the cases of symmetric (or nearly symmetric) loops in this domain, this procedure effectively promises a least squares minimization of any Bouc-Wen loop with its corresponding Preisach loop.

3.2.2   Use of Artificial Neural Networks

The least squares minimization method works well. However, an alternative approach to consider is the conversion of Bouc-Wen into Preisach parameters via an ANN. There are a couple advantages that could arise from using an ANN. Namely, with a pre-built library of input and output values (of matching Bouc-Wen and Preisach parameters, respectively), the database can be easily shared among fellow researchers to work into their own code instead of everybody using different methods for optimization. Further, the ANN, once trained, works essentially instantaneously.

To build the ANN, there needs to be a library of input and output values for the ANN. This is accomplished by running the least squares minimization approximately 750 times. There needs to be a fairly large database for the ANN to train properly because of the large amount of permutations the Bouc-Wen values can take. Once this database is generated, the ANN is trained. For the ANN, a hidden layer size is chosen to be 20 neurons. This is optimized using a trial-and-error approach. With a black box approach such as this, there is no exact or analytical method for determining the proper amount of neurons or hidden layers. Thus, the ANN consists of an input vector of 7×750 Bouc-Wen parameters, a hidden layer consisting of 20 neurons, and an output layer consisting of 6×750 Preisach parameters. Further, the ANN needs a certain ratio of the database to train, validate, and test. For this study, the standard $70/15/15$ ratio for training, validating, and testing was employed, as there was no sufficient reason to deviate.

After the ANN is trained, it can be validated by generating a random (within the prescribed bounds) set of Bouc-Wen values. The Bouc-Wen values are generated and inputted into the ANN, the ANN solves for the Preisach values, and then both the original Bouc-Wen model and fitted Preisach model are graphed for comparison. Figure 3.2, Table 3.5, and Table 3.6 show the results of this endeavor.
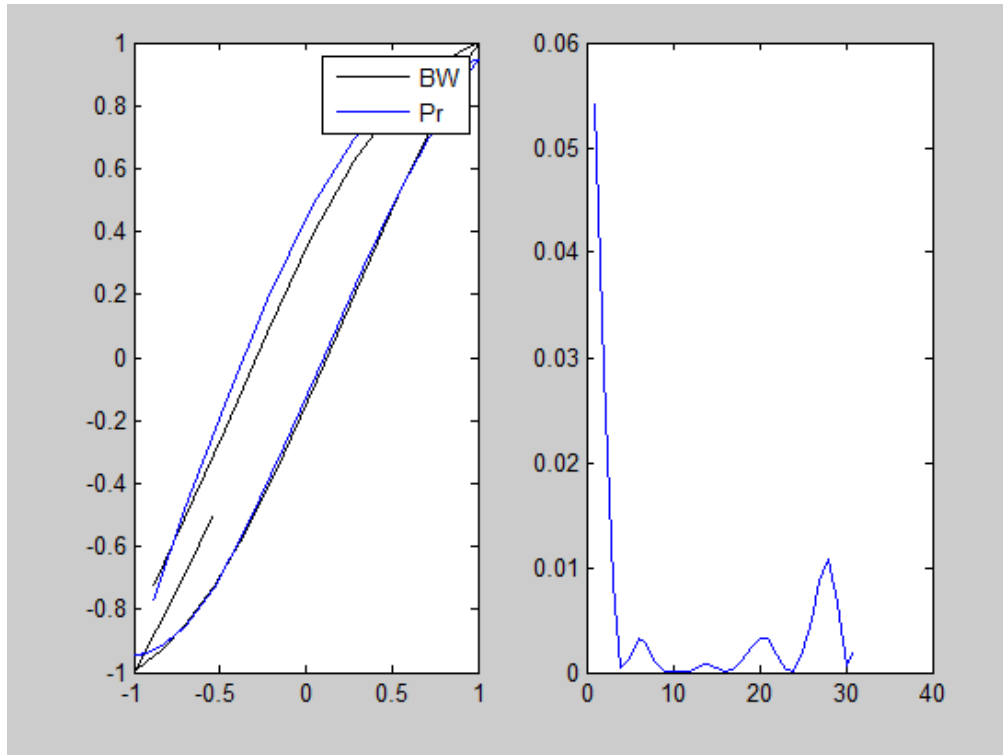
Figure 3.2: Fitted Preisach values via ANN

Parameter	Value
α	0.2988
β	3.2301
γ	1.6160
ζ	0.0629
ω_n	3.2122
A	0.8742
n	1.9876

Table 3.5: Sample Bouc-Wen values with ANN

Parameter	Value
μ_α, μ_β	$0.9527, -0.7868$
$\sigma_\alpha, \sigma_\beta$	$1.3123, 1.2121$
ρ	0.8658
k	5.9072

Table 3.6: Fitted Preisach values with ANN

Thus, under certain conditions, the ANN works quite well. However, given the highly nonlinear and difficult-to-predict nature of the Bouc-Wen model, the ANN does not work quite as well when considering more abrupt types of loops (such as incredibly square or "S" shaped ones). Still, it has its use in the conversion from one model to another.

3.3   On the Conversion of Preisach Parameters into Bouc-Wen Parameters

Although it is the opinion of this author that, due to the Preisach model's versatility in fitting different types of loops and ability to be analyzed via methods such as stochastic averaging, it is an interesting exercise to perform the conversion the other direction to prove the versatility of the ANN method. Under the same conditions, the Preisach model loop can be converted effectively into the Bouc-Wen model loop.

The same procedure as before is adopted with the least squares method. The only change is that the input is the vector of the Preisach parameters and the output is the vector of the Bouc-Wen parameters. The results of a randomized trial are shown in Figure 3.3, Table 3.7, and Table 3.8.
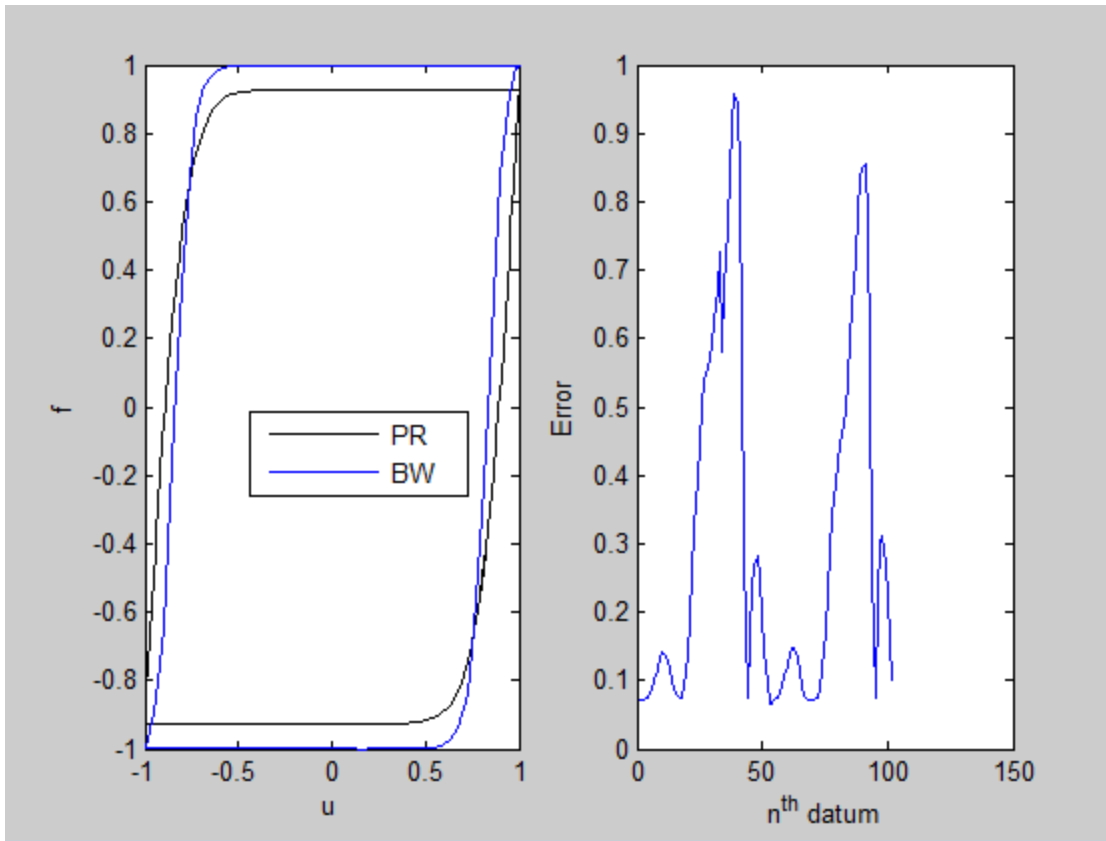
Figure 3.3: Fitted Bouc-Wen parameters to a Preisach loop

Parameter	Value
$|\mu|$	1.0436
σ	0.1832
ρ	0.0243
k	5.7559

Table 3.7: Fitted Preisach values with LSQ

Parameter	Value
α	0.0501
β	40.8387
γ	2.5755
ζ	0.1832
ω_n	1.9621
A	0.9114
n	1.9307

Table 3.8: Fitted Bouc-Wen values with LSQ

This exercise has shown that, under proper conditions, the Bouc-Wen model can fit a fairly wide range of loops. Its success depends largely on the choice of an initial guess, as, with seven parameters, the Bouc-Wen model can become easily trapped in a local minimum before adequate convergence. The arrival at a satisfactory initial guess is related directly to knowing how each parameter affects the overall loop, which is the subject of the following chapter.

3.4   Summary

Through the investigation above, it is shown that the ANN works well under strict circumstances. There are a few major factors that explain the success of the ANN. First, the ANN must, of course, have enough iteration to develop confident weighing nodes. Second, it must be trained on a specific set of data for a certain kind of hysteresis loop. It is easier for the code to deal with a relatively limited series of loops for one library, due to the high amount of

variation that can occur with seven Bouc-Wen parameters. Different libraries can be built for different kinds of hysteresis loops, such as those exhibiting hardening versus softening trends.

Chapter 4

Revisiting Preisach and Bouc-Wen Parameter Effects

4.1   Preliminary Remarks

For many inverse modeling scenarios, an adequate starting estimate for the parameters of either model is critical. Without a good starting guess, the convergence for least squares can get stuck in a local minimum and never converges to the desired accurate degree. In the best case, it will converge slower than it otherwise can. In the worst case, it will fail to converge at all. This is especially true with the Bouc-Wen model, for it is balancing seven parameters as opposed to the Preisach model's four (with two extra being symmetric) parameters. Thus, to make a good initial estimate, becoming intimately aware with how each parameter affects each model is critical.

4.2   Preisach Parameters

As discussed in previous sections, the Preisach model is comprised of the following six parameters:

$$\mu_a, \mu_b, \sigma_a, \sigma_b, \rho \ (or \ r), and \ k$$

where the parameters refer to the mean of the ascending loop, mean of the descending loop, standard deviation of the ascending loop, standard deviation of the descending loop, the distribution correlation, and the scaling constant, respectively.

To accurately describe the effect of one of the parameters, the other parameters must be held constant. There are also a couple restrictions based upon this analysis of the Preisach model:

1) $\mu_a = -\mu_b$ (4.1)

2) $\sigma_a = \sigma_b$ (4.2)

These are enforced to keep the loop symmetric, which is a common assumption in many hysteresis cases [18, 19, and 22]. The first case that will be investigated is the effect of the mean on a loop. Below is an output with changing mean values with the other parameters held constant at $\sigma_a = \sigma_b = 1, \rho = 0$, and $k = 2$.
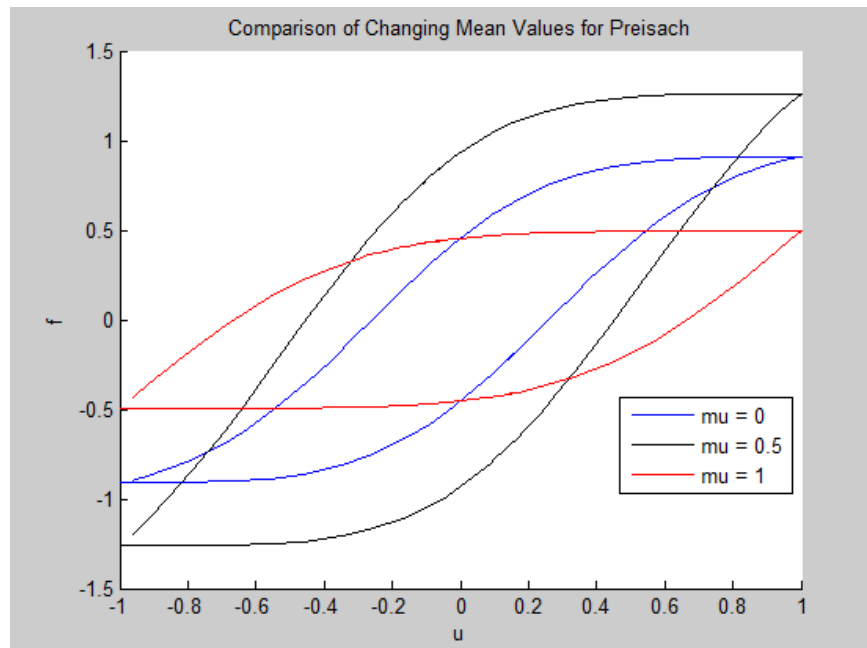
Figure 4.1: Preisach model with changing mean

In Figure 4.1, having a higher mean value leads to a more square loop, while having a lower mean value leads to a more vertical loop. Even more importantly for this study, note that the spot where the restoring force rises above the x-axis is pushed farther outwards with an increasing

mean. Next, the same investigation can be performed with the standard deviation changing. The output is shown in Figure 4.2, with all other parameters the same as before ($\mu = 0.5$).
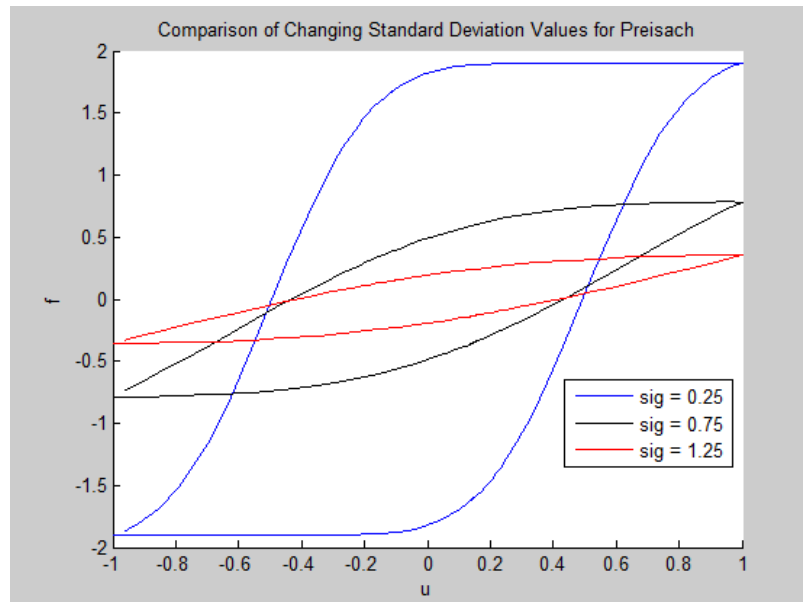
Figure 4.2: Preisach model with changing standard deviation

As shown, increasing the standard deviation makes the loop more compressed. Finally, the same investigation can be done with the correlation, as seen in Figure 4.3.
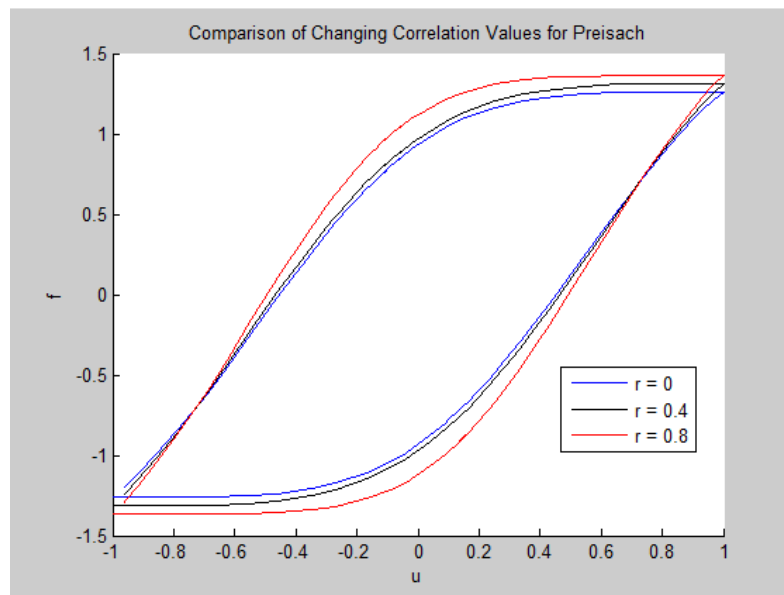
Figure 4.3: Preisach model with changing correlation

The correlation has a minor effect on a loop. It is used more as a fine tool than defining the type of loop. The higher the correlation becomes, the more drastic of a vertical increase it has. The correlation would affect the symmetry more drastically for the loop if the input itself was not symmetric. In these cases, it is a sinusoidal input, so altering the correlation has minimal effect. The scaling coefficient k has the obvious effect of scaling the vertical restoring force to a particular domain.

The key to fitting a wide variety of loops with the Preisach model lies in the accurate initial estimate for the mean. Currently, for all kinds of loops considered, having the values

$$\sigma = 0.5, \rho = 0, k = 2$$

set initially leads them to converge in all studied cases. To obtain an accurate guess for the mean, where the loop crosses the x-axis (both ascending and descending) must be investigated. Essentially, whatever the displacement is when the loop crosses $f = 0$ is what the initial mean guess should be. An example is shown in Figure 4.4.
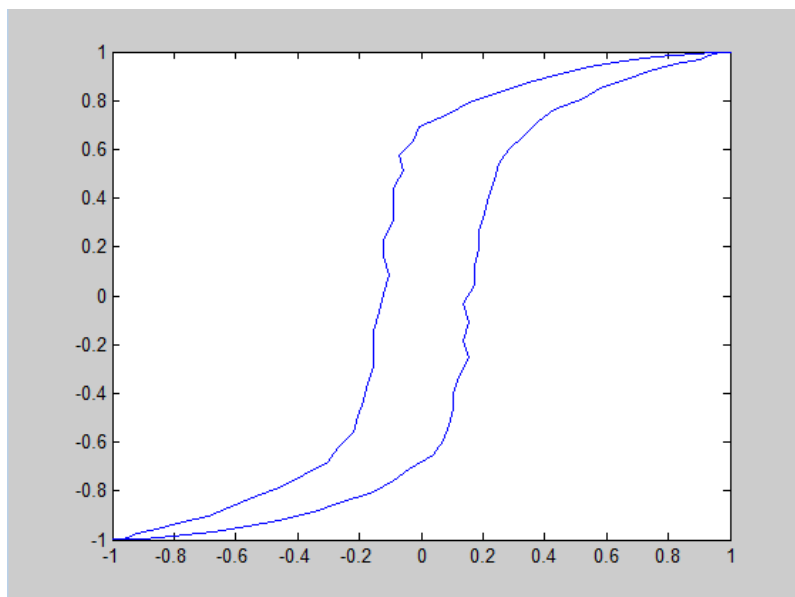
Figure 4.4: Sample experimental loop

With a more vertical S-shaped loop like this, the initial guess for the mean should be in the range of around 0.1. After performing the fitting procedure, the Preisach model yields the fit and parameters shown in Figure 4.5 and Table 4.1.
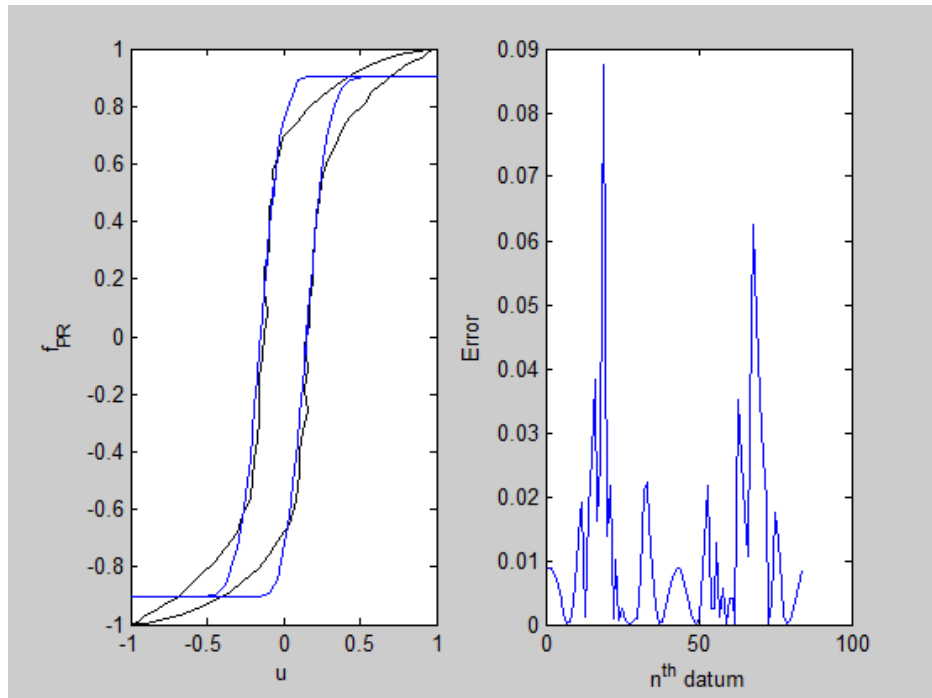
Figure 4.5: Preisach model fitted to sample experimental loop

Parameter	Value
$|\mu|$	0.1364
σ	0.1204
ρ	-0.34
k	0.9838

Table 4.1: Fitted Preisach values towards sample experimental loop

Thus, the Preisach loop's fitting procedure proves quite versatile. The crux of the convergence lies with the accurate estimation of the mean. After that, all of the parameters converge within only several iterations. A helpful heuristic that arises for μ is that, generally, the loop will cross

the horizontal axis close to $|\mu|$ for both the ascending and descending branches. Thus, the author's suggestion for an estimate mean value is to find where the loop crosses the x-axis (assuming a symmetric loop) and establish $|\mu_0|$ from there.

4.3   Bouc-Wen Parameters

As stated in *Chapter 2*, the parameters associated with the Bouc-Wen model are the rigidity ratio α, the linear elastic viscous damping ratio ζ, the pseudo-natural frequency of the system ω_n, the hysteresis amplitude controlling parameter A, and the hysteresis loop shape controlling parameters β, γ, and n.

There are some inherent difficulties when it comes to fitting the Bouc-Wen model to a wide range of hysteretic data, partially because of the simultaneous error minimization with seven parameters. This often leads to local minimums in the least squares approach, which may or may not be a good overall fit. Figures 4.6 through Figure 12 show how each parameter affects the overall shape of the loop. In each scenario, there is one parameter changing, while the others hold the following values, chosen partially arbitrarily for creating a medium-sized loop:

$$\alpha = 0.05, \beta = 40.85, \gamma = 0.3, \zeta = 0.98, \omega_n = 1.05, A = 0.9, n = 4$$
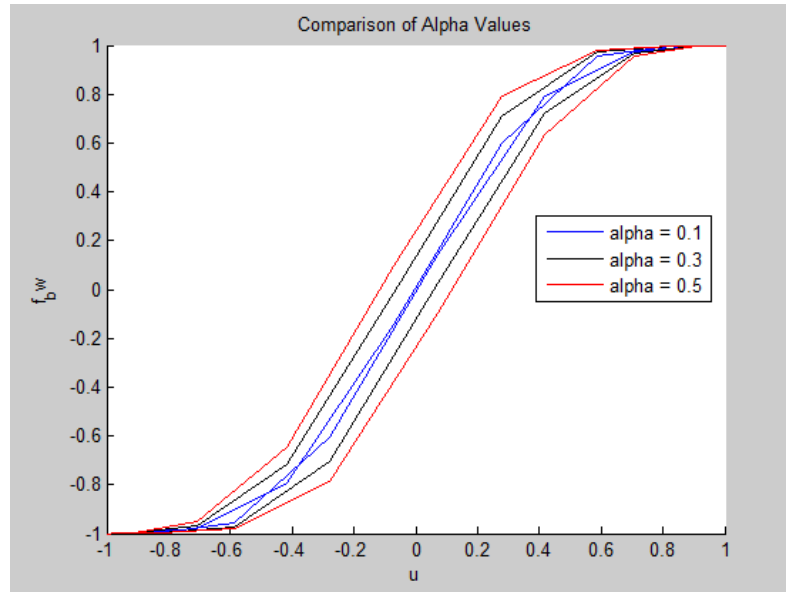
Figure 4.6: Bouc-Wen model with changing α
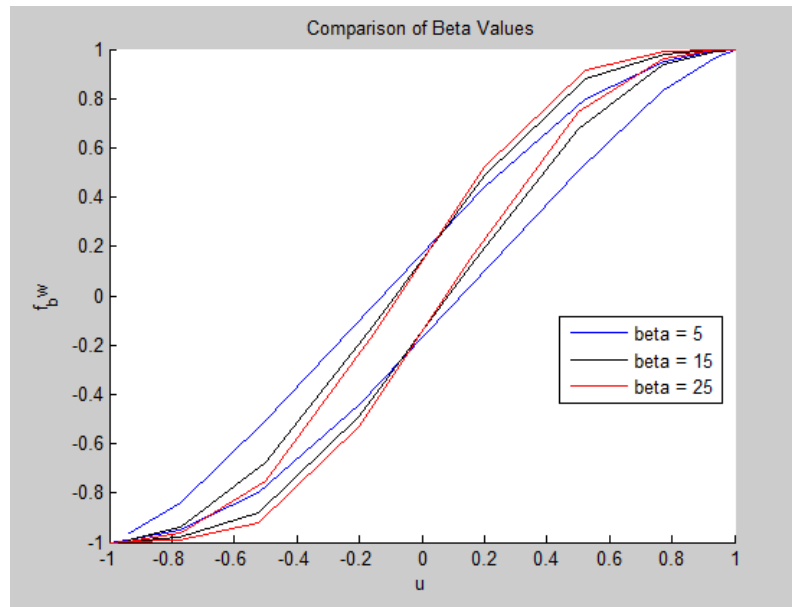
Figure 4.7: Bouc-Wen model with changing β
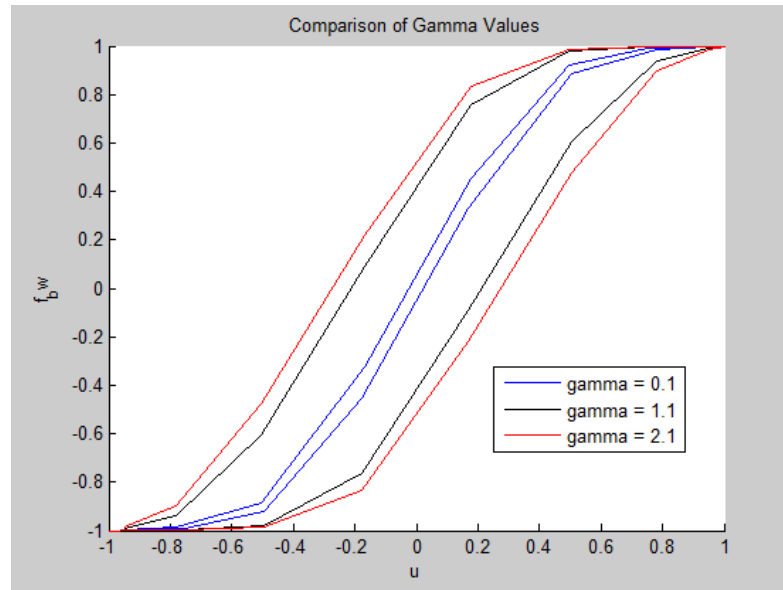
Figure 4.8: Bouc-Wen model with changing γ
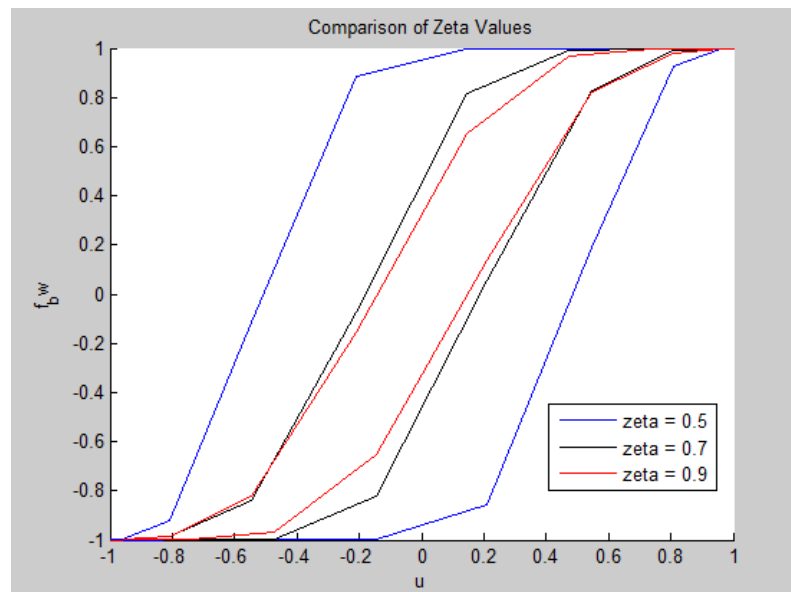
Figure 4.9: Bouc-Wen model with changing ζ
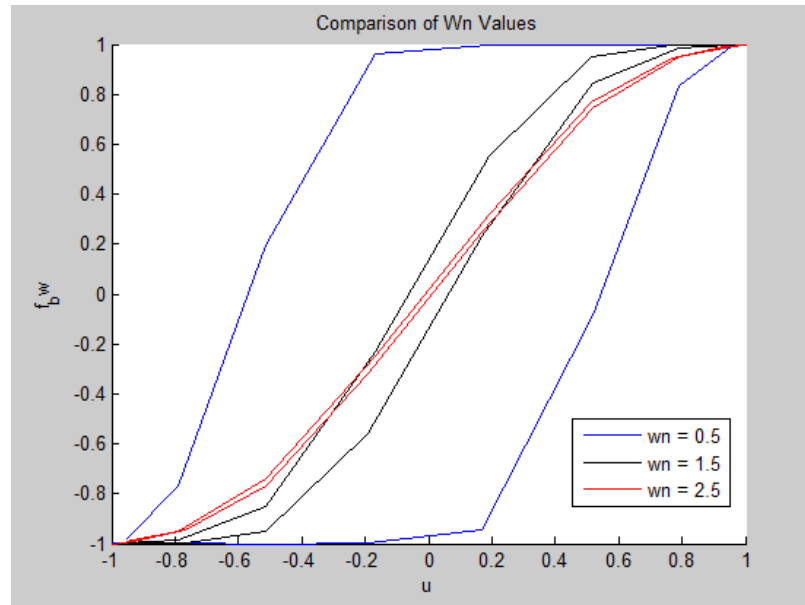
Figure 4.10: Bouc-Wen model with changing ω_n
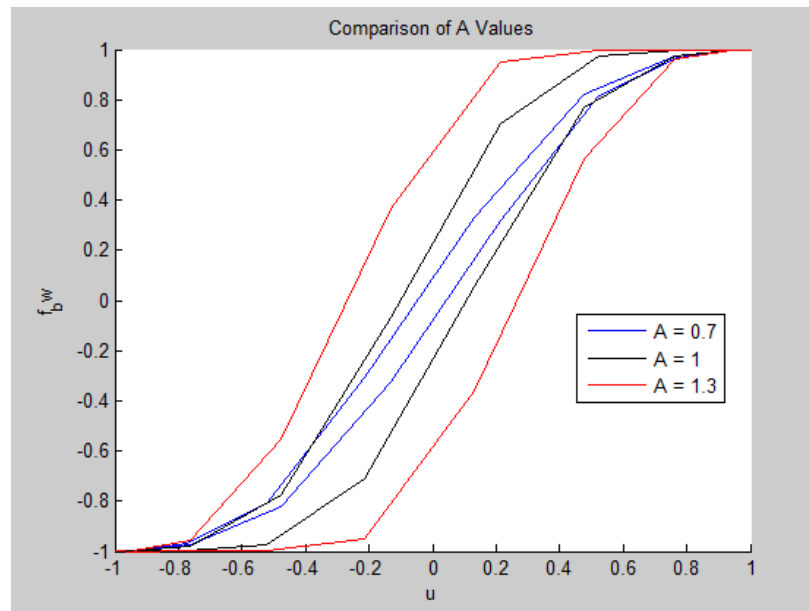
Figure 4.11: Bouc-Wen model with changing A
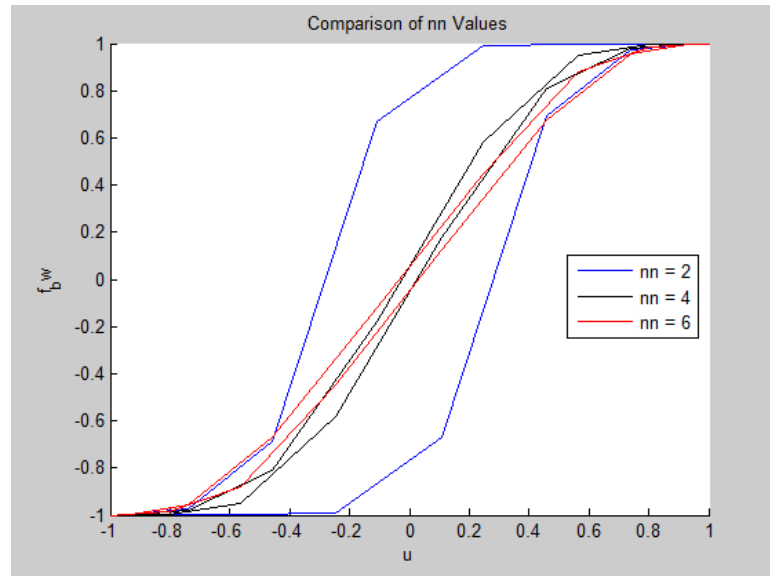
Figure 4.12: Bouc-Wen model with changing n

From all of these graphs modifying each parameter, the following trends can be noticed:

As each parameter increases	Effect
α (rigidity ratio)	Loop grows wider
β (loop controlling parameter)	Loop grows more vertical and less slanted
γ (loop controlling parameter)	Loop grows wider
ζ (damping ratio)	Loop width decreases
ω_n (natural frequency)	Loop slants more to the right and width decreases
A (amplitude controlling parameter)	Width increases
n (loop controlling parameter)	Loop becomes more narrow

Table 4.2: Bouc-Wen parameter effects

There is an interesting trend to note for the parameter β. This parameter directly affects whether or not the hysteresis loop exhibits hardening or softening hysteretic behavior [48]. Figure 4.13 captures this behavior.
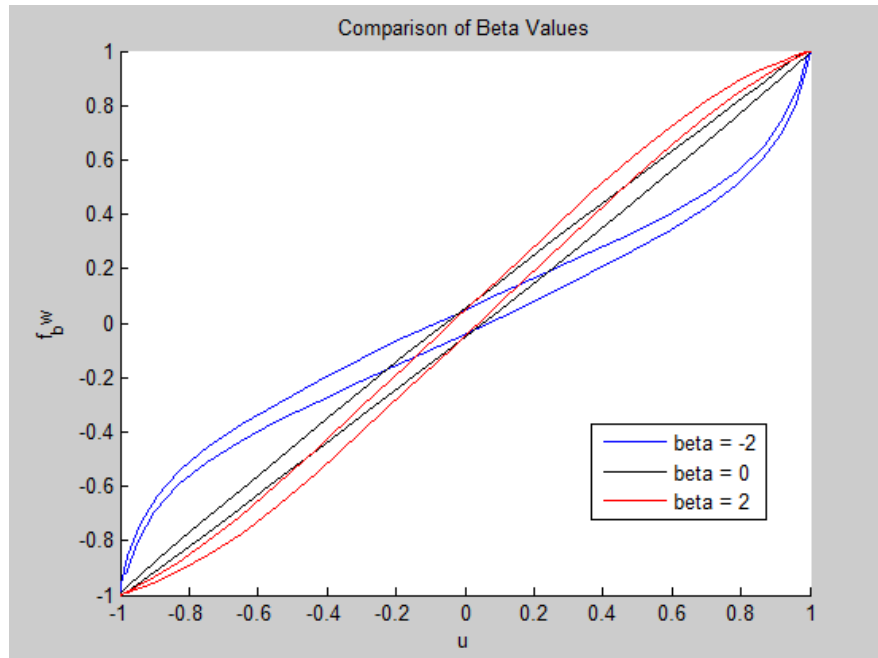
Figure 4.13: Bouc-Wen model with negative and positive β

As shown, when $\beta < 0$, the model experiences softening hysteretic behavior. When $\beta = 0$, the model experiences linear hysteretic behavior. When $\beta > 0$, the model experiences hardening hysteretic behavior.

These results are in good agreement with the existing literature by Solomon and Charalampakis [48, 49]. Taking into consideration these trends is critical for the production of an adequate starting guess for least squares convergence. Below is an example of a square loop being fitted by the Bouc-Wen model with a relatively high degree of accuracy. For a loop of this kind with extremely high width, the initial starting guess must have some of the following characteristics:

I. Larger α,

II. Large β,

III. Large γ,

IV. Small ζ,

V. Small to medium ω_n,

VI. Medium to large A, and

VII. Smaller n

With these guidelines, the following set of parameters is adopted:

$$\alpha = 0.05, \beta = 40.85, \gamma = 10.8, \zeta = 0.18, \omega_n = 2, A = 0.9, n = 1.9$$

After convergence, the Bouc-Wen loop is produced alongside the data as shown in Figure 4.14.
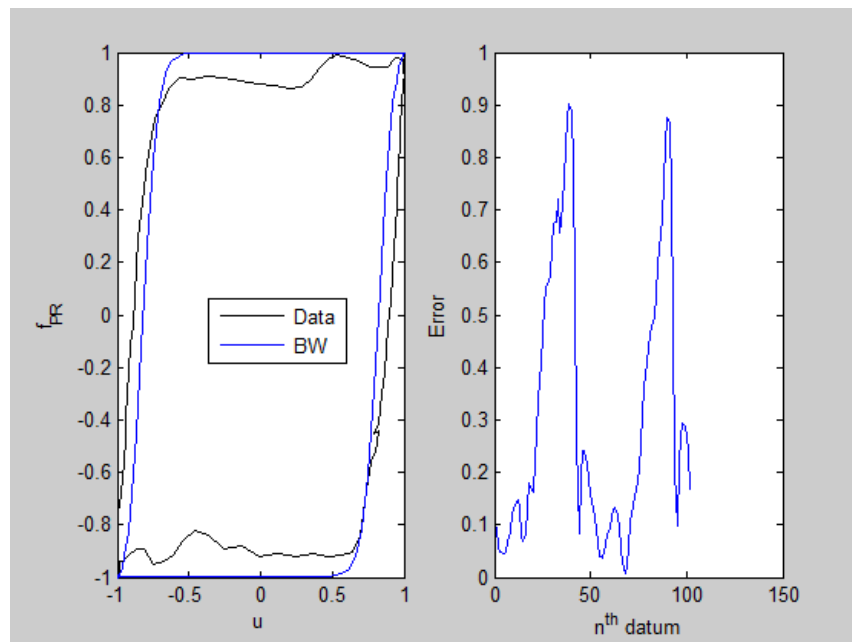
Figure 4.14: Fitted Bouc-Wen loop with experimental data

It is seen that there is a moderately good fit is achieved using the Bouc-Wen model (with a root mean square error/point value of 0.3), provided a reasonable starting guess. The fitted parameters are:

Parameter	Value
α	0.022
β	40.6962
γ	2.6248
ζ	0.1729
ω_n	1.9903
A	0.894
n	1.9738

Table 4.3: Fitted Bouc-Wen parameters with experimental loop

4.4   Summary

With this knowledge of how each parameter specifically affects the shape and size of the hysteresis loop for both the Preisach and Bouc-Wen models, more confident analysis is ensured when applying these principles towards an initial guess for a convergence algorithm. These principles can effectively be applied towards experimental data, and a performance study can be evaluated on the fitting of both models towards experimental data with the assurance of convergence via adequate initial estimates.

Chapter 5

Performance of Preisach Parameters and Bouc-Wen Parameters on Experimental Data

5.1   Preliminary Remarks

One of the main reasons for understanding the inner workings of the Preisach model and the Bouc-Wen models of hysteresis is to apply the models in conjunction with experimental data. With finely calibrated models, the identification problem for many types of hysteresis loops' behavior can be captured. One of the focuses of the thesis is to investigate how the different models fare against matching experimental data. In this study, sample sets of hysteresis data are generously supplied by the Air Force Research Lab (AFRL) in conjunction with Dr. Abdellah Lisfi's research group at Morgan State University. These loops are analyzed via the Preisach model and Bouc-Wen model. The models solve the identification problem for the experimental data with minimized error via LSQ.

5.2   Comparison of Preisach and Bouc-Wen Models

Using the mathematical techniques outlined in *Chapter 2* and the guidelines for choosing the initial guess for the parameters outlined in *Chapter 4*, the two models can be juxtaposed against each other. Shown in Table 5.1 and Table 5.2 are the fitted parameters for the five different data sets, looking at epitaxial Cobalt ferrite film with in-plane anisotropy at different angles supplied by AFRL. Next, in Figure 5.1, the fitted parameters are plotted against the experimental data set

for a visual comparison. Note that all error calculations are accomplished using root mean square

error.

Case #	$|\mu|$	σ	ρ	k	Error/Point
1	0.8316	0.503	0.3006	279.5913	0.0066
2	0.3642	0.0763	0.9918	0.9451	0.0071
3	1.0436	0.1832	0.0243	5.7559	0.0015
4	3.1717	1.6929	0.2371	261.2788	0.0050
5	0.1364	0.1204	-0.3404	0.9839	0.0111

Table 5.1: Fitted Preisach parameters and error

Case #	α	β	γ	ζ	ω_n	A	n	Error/Point
1	0.0948	16.0314	0.293	0.9829	1.0328	0.9405	3.9495	0.2855
2	0.0175	40.927	1.8076	0.1959	1.9373	0.9122	4.8867	0.2252
3	0.022	40.6962	2.6248	0.1729	1.9903	0.894	1.9738	0.3106
4	0.201	5.9996	4.0996	0.8505	3.9998	0.9999	1.0007	0.4792
5	0.0979	11.2206	0.2638	0.4841	1.4805	0.9581	2.4432	0.4654

Table 5.2: Fitted Bouc-Wen parameters and error
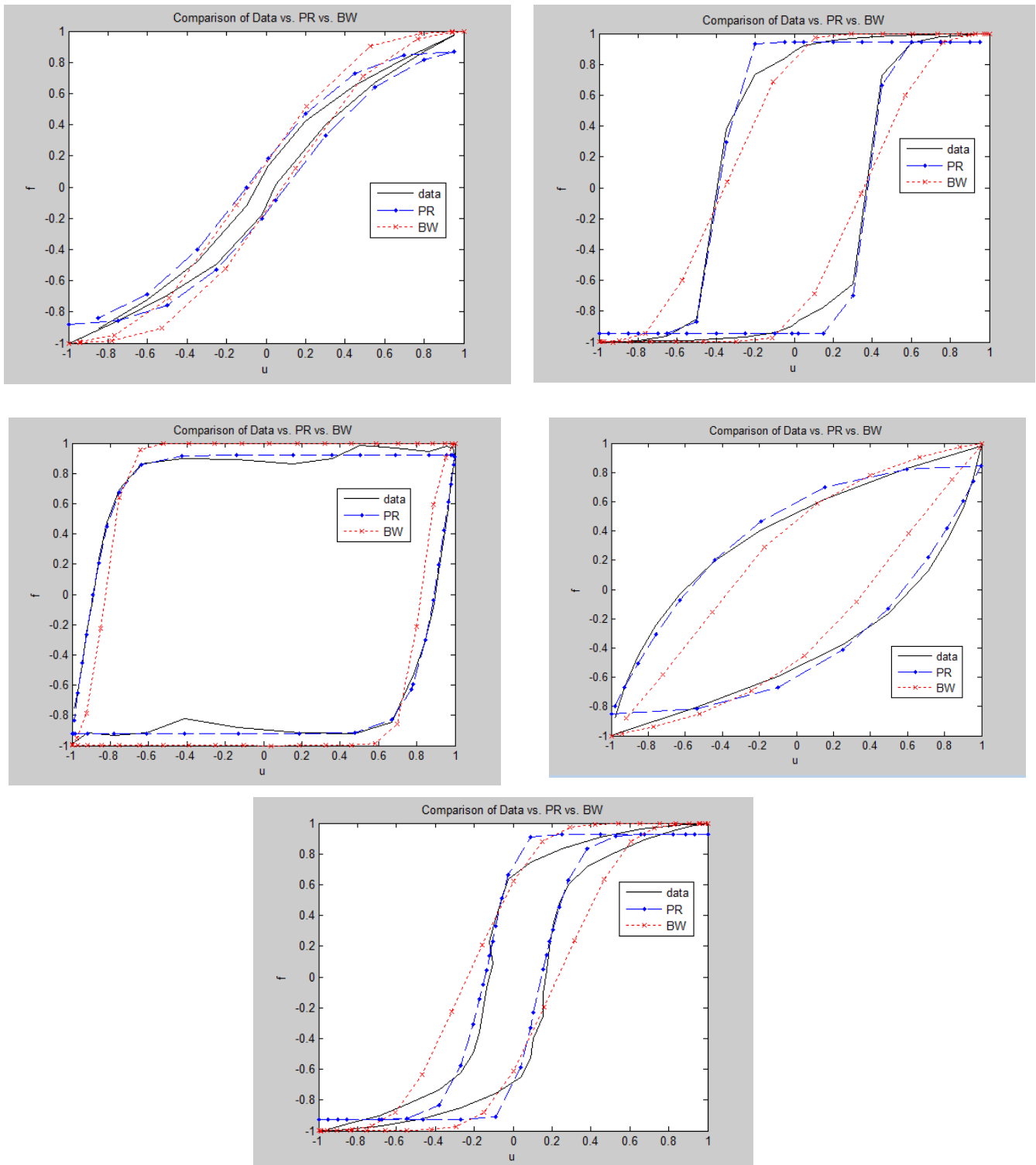
Figure 5.1: Hysteresis loops comparing Preisach and Bouc-Wen models vs. experimental data;

Cases 1-5

5.3   Discussion of Fits

There are a few important trends to note when evaluating the parameters of best fit for solving the identification problem via Preisach formalism and the Bouc-Wen differential equation methods.

First, a trend arises in all the experimental data sets. Specifically, the Preisach model fits more accurately than the Bouc-Wen model. This is true for Case 1 through Case 5. The Preisach model seems to be more effective in fitting different types of models as well. In particular, the Bouc-Wen model fit has more difficulty fitting loops in situations like Case 2, Case 4, and Case 5. In Case 2 and Case 5, the error is relatively large because of the "s" shaped nature of the hysteresis loop. The Bouc-Wen model "struggles" to rise so rapidly when the applied displacement is around zero (the middle of the loading or unloading cycle). Due to the Preisach model's flexibility in assigning the standard deviation value, it can rapidly rise in the middle of the cycle. There is no proper analog in the Bouc-Wen model; it is thus more difficult with fitting these loops. In a similar fashion, the Bouc-Wen model struggles to minimize the error in Case 4 because of the width of the loop. It can adjust to loops with very large area (like Case 3) with fine tuning, but it cannot adjust as well to the loop in Case 4 that has larger area but does not rise rapidly at the end (hysteretic softening).

Second, note that the error comparison between the Preisach and Bouc-Wen models is not quite a one-to-one comparison. By the nature of the Bouc-Wen model, it is based in a series of differential equations. Thus, the output in the subroutine ODE45 in MATLAB that is produced has its own set of data in both axes. In contrast, the Preisach model matches the displacement

data from the experimental set directly. Therefore, the Bouc-Wen model error is associated with the u and f axes, whereas the Preisach model is only concerned with the f axis. This is why Table 5.1 and Table 5.2 are accompanied by Figure 5.1; the visual representation helps understand the competency of the fit as much as the sum of the error.

Third, an inherent difficulty lies in the sheer amount of parameters that the LSQ approach tries to minimize with the Bouc-Wen model. The Preisach model is concerned with fitting four variables to the sample set. In contrast, the Bouc-Wen model is concerned with fitting seven variables. With the variables being interdependent in the differential equations, it is easy for the LSQ algorithm to fall into local minimums. Thus, it is critical to follow the guidelines outlined at the end of *Chapter 4* for the Bouc-Wen model parameters' initial estimate. However, this difficulty is not entirely erased via an appropriate starting guess; a wide yet specific margin for the upper and lower bounds for the Bouc-Wen parameters must be ensured.

5.4   Summary

Through the analysis in the section above, it is concluded that the Preisach model is, in general, better at fitting the wide variety of loops that the hysteresis phenomenon can exhibit. Further, certain sources suggests that the Preisach model shows promise in applications such as stochastic averaging and equivalent linearization, making it a more desirable model in applications regarding stochastics and dynamic response [21, 22, 50, and 51]. Nonetheless, the Bouc-Wen model does exhibit some appealing features. For one, it is a faster method, albeit slightly. The differential equation basis for the method is computationally less demanding than building the Preisach half-plane. Further, there are modifications to the Bouc-Wen model, such as the Bouc-

Wen-Baber-Noori model, which more accurately deals with the system identification of hysteresis loops subject to pinching [52 – 57].

Chapter 6

System Identification of Hysteresis Loops Using Transitional Markov Chain Monte Carlo Based Bayesian Approach

6.1   Preliminary Remarks

An interesting application of fitting experimental (especially noisy) data involves the use of Bayesian statistics. Bayesian inference is a statistical method in which, as new data are acquired, Bayes' rule is used to update the probability estimate for a hypothesis. There is interest in model updating techniques due to the broad application and probability based approach. Among the model updating techniques, Bayesian inference techniques do not just find a single model but a probability distribution set of models whose predictions are weighted by the probabilities of these models conditional on the measured data [58–63]. These Bayesian model updating techniques are robust and suitable to modeling nonlinear phenomena such as hysteresis due to their ability to consider more than one model when there may be more than one solution. Further, Bayesian techniques in this way can prove useful when applied to loops affected by white noise corruption.

The Markov Chain Monte Carlo (MCMC) method simulates random samples from a specified target probability distribution function (PDF) that can be evaluated up to a scaling constant. Thus, from the Bayesian point of view, the target PDF is the posterior PDF, and the scaling

constant is denoted as the model evidence. Essentially, MCMC works by simulating a Markov chain with a stationary PDF equal to the target PDF. In the literature, the most popular algorithm for the MCMC method is the Metropolis-Hastings algorithm [64, 65]. An important attribute of the Metropolis-Hastings algorithm is that it does not calculate the model evidence because the PDF is only evaluated up to a scaling constant.

However, the MCMC method is subject to a few critical limitations. It cannot evaluate the model evidence – the likelihood of the observed data given the chosen model. This is the greatest limitation. The proposal PDF determines how far the Markov chain sample can jump to the next candidate sample. With wide PDFs, the candidate has a larger chance of being rejected, as it could be a low probability region. On the other hand, with narrow PDFs, the candidate has a greater chance of being accepted, but consecutive Markov chain samples will have the undesirable quality of being highly correlated, along with the possibility that the proposed PDF does not adequately capture the behavior of the variable. This is especially the case when the target PDF is highly dimensional or has highly correlated random variables [66]. There is another issue with convergence in that it is uncertain how many Markov chain samples are required to adequately cover the target PDF. There is no guarantee that a limited number of Markov chain samples can cover the main region of the target PDF. There is literature dealing with this issue, but it adds complexity towards knowing the target PDF [67].

To solve these problems, a modified version of the MCMC method was proposed in 2007 and titled the Transitional Markov Chain Monte Carlo (TMCMC) method [68]. It works as an amalgamation of the Metropolis-Hastings algorithm with the sampling-importance-resampling

method [69-70]. It is a method free of tuning; there is no need to specify the proposal PDF, and the convergence issues are minimized. One of the key ideas in the TMCMC method is to circumvent sampling directly from the difficult-to-determine target PDF and to sample from a series of intermediate PDFs that eventually converge to the target PDF.

6.2   TMCMC Theory

To appreciate the TMCMC method, some related mathematical background is required. First, let M be the assumed probabilistic model class for the target system, θ be the uncertain model parameters, and D be the measured data from the system. The goal of the Bayesian model updating is to sample the posterior PDF of θ conditioned on D. This is shown in Eq. (6.1).

$$f(\theta|M,D) = \frac{f(D|M,\theta) * f(\theta|M)}{f(D|M)} = \frac{f(D|M,\theta) * f(\theta|M)}{\int f(D|M,\theta) * f(\theta|M) * d\theta}. \qquad (6.1)$$

In Eq. (6.1), $f(\theta|M)$ is the prior PDF of θ, $f(D|M,\theta)$ is the likelihood function of D, given θ, and $f(D|M)$ is the evidence of M. Simulation based methods are valuable for Bayesian model updating for their use in obtaining samples from $f(\theta|M,D)$, which can estimate any quantity of interest $E(g|M,D)$ according to the Law of Large Numbers.

$$E(g|M,D) \approx \frac{1}{N} \sum_{k=1}^{N} g(\theta_k). \qquad (6.2)$$

In Eq. (6.2), $\theta_k, k = 1, 2, \dots, N$ is the set of N samples from $f(\theta|M, D)$. Consider the following equation in Eq. (6.3).

$$f(\theta|M, D) \; \alpha \; f(\theta|M) * f(D|M, \theta).$$

(6.3)

Sampling from $f(\theta|M, D)$ using the Metropolis-Hastings algorithm with the sampling-importance-resampling method can be difficult because the geometry of the likelihood $f(\theta|M, D)$ cannot be known beforehand. Instead, intermediate PDFs that converge towards the target PDF $f(\theta|M, D)$ must be constructed. Consider a series of intermediate PDFs in Eq. (6.4).

$$f_j(\theta) \; \alpha \; f(\theta|M) * f(D|M, \theta)^{p_j}$$

(6.4)

$$j = 0, 1, \dots, m \quad 0 = p_0 < p_1 < \cdots < p_m = 1$$

Also, note that $f_0(\theta) = f(\theta|M), f_m(\theta) = f(\theta|M, D)$.

Although the geometry changes from $f(\theta|M)$ to $f(\theta|M, D)$ can be drastic, the change between the adjacent intermediate PDFs is small. Thus, the algorithm can efficiently obtain samples from $f_{j+1}(\theta)$ based on samples from $f_j(\theta)$. This sampling scheme uses the $f_j(\theta)$ samples to estimate the PDF as a kernel density function (KDF), which is a mixture of weighted Gaussians centered at the samples. This resulting KDF is taken as the proposal PDF of the Metropolis-Hastings algorithm to draw samples for the next iteration. Doing this a number of times will eventually yield the $f(\theta|M, D)$ samples. This process describes the modified version of the Metropolis-Hastings method.

The TMCMC algorithm takes a different approach to the $f_{j+1}(\theta)$ based on samples from $f_j(\theta)$, using a resampling method instead of the KDF approach. It consists of a series of resampling stages, with each stage doing the following: given N_j samples from $f_j(\theta)$ denoted by $\{\theta_{j,k}: k = 1, \dots, N_j\}$, obtain samples from $f_{j+1}(\theta)$, denoted by $\{\theta_{j+1,k}: k = 1, \dots, N_{j+1}\}$. With the samples $\{\theta_{j,k}: k = 1, \dots, N_j\}$ from $f_j(\theta)$, the plausibility weights of the samples can be calculated.

$$w(\theta_{j,k}) = \frac{f(\theta_{j+1,k}|M)f(D|M,\theta_{j,k})^{p_{j+1}}}{f(\theta_{j,k}|M)f(D|M,\theta_{j,k})^{p_j}} = f(D|M,\theta_{j,k})^{p_{j+1}-p_j} \qquad (6.5)$$

$$for \; k = 1, \dots, N_j.$$

Next, the uncertain parameters can be resampled according to the normalized weights. Let

$$\theta_{j+1,k} = \theta_{j,l}, w.p. \; \frac{w(\theta_{j,l})}{\sum_{l=1}^{N_j} w(\theta_{j,l})} \; k = 1, \dots, N_{j+1}.$$

Here, w.p. stands for "with probability" and l is the dummy index. If N_j and N_{j+1} are large, $\{\theta_{j+1,k}: k = 1, \dots, N_{j+1}\}$ will approach the distribution of $f_{j+1}(\theta)$. Furthermore, the expected value of $w(\theta_{j,k})$ is denoted in Eq. (6.5).

$$E[w(\theta_{j,k})] = \int w(\theta) * f_j(\theta)d\theta \qquad (6.5)$$

$$= \int f(D|M,\theta_{j,k})^{p_{j+1}-p_j} * f_j(\theta)d\theta$$

$$= \int f(D|M,\theta_{j,k})^{p_{j+1}-p_j} * \frac{f(\theta|M)f(D|M,\theta)^{p_j}}{f(\theta|M)f(D|M,\theta)^{p_j}d\theta}$$

$$= \frac{\int f(\theta|M)f(D|M,\theta)^{p_j+1}d\theta}{\int f(\theta|M)f(D|M,\theta)^{p_j}d\theta}.$$

Thus, $\sum_{k=1}^{N_j} w(\theta_{j,k})/N_j$ is the unbiased estimator for $\frac{\int f(\theta|M)f(D|M,\theta)^{p_{j+1}}d\theta}{\int f(\theta|M)f(D|M,\theta)^{p_j}d\theta}$.

With probability $w(\theta_{j,k})/\sum_{l=1}^{N_j} w(\theta_{j,l})$, a Markov chain sample in the kth chain is generated using a Gaussian proposed PDF centered at the current sample of the kth chain with a covariance matrix equal to the scaled version of the estimated covairance matrix of $f_{j+1}(\theta)$.

$$\sum_j = \beta^2 \sum_{k=1}^{N_j} w(\theta_{j,k}) \left\{ \theta_{j,k} - \left[\sum_{k=1}^{N_j} w(\theta_{j,l})\theta_{j,l} / \sum_{k=1}^{N_j} w(\theta_{j,l}) \right] \right\} \qquad (6.6)$$

$$* \left\{ \theta_{j,k} - \left[\frac{\sum_{k=1}^{N_j} w(\theta_{j,l})\theta_{j,l}}{\sum_{k=1}^{N_j} w(\theta_{j,l})} \right] \right\}^T .$$

In Eq. (6.6), β is the scaling factor and $\sum_j =$ the product of β^2 and the estimated covariance of $f_{j+1} = \theta$. Choosing the β value is important for ensuring a smaller rejection rate as well as making large enough Markov chain jumps. Through much of the literature, it is found that 0.2 works well for this value [71]. Choosing the proper p_j values is also important. If these values change too slowly, the amount of intermediate PDFs will be huge. If these values change too quickly, the transition between the adjacent PDFs will not be smooth. Figure 6.1 shows a visualization of the TMCMC algorithm.
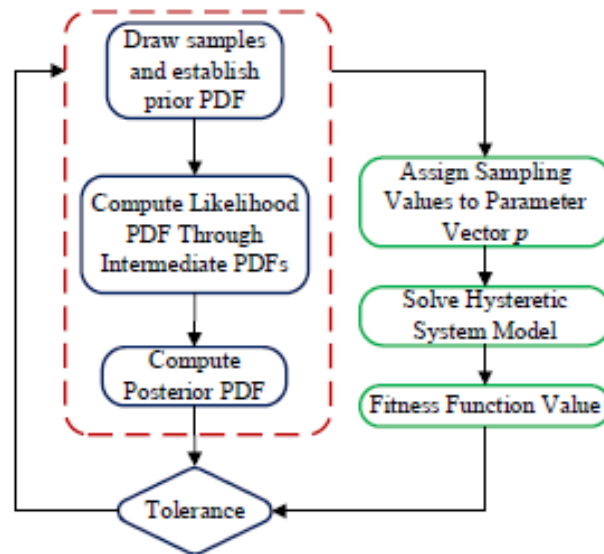
Figure 6.1: TMCMC implementation strategy

The algorithm evolves by first assuming the PDFs for every variable is uniform. In this stage, $p_0 = 0$. Via Bayesian inference and the TMCMC probability simulations, the samples eventually populate the high probability region of the posterior Gaussian PDFs close to the true model parameters at the last stage, where $p_m = 1$.

6.3   TMCMC with the Preisach Model

The TMCMC method has been applied with some success towards the Bouc-Wen model [72-73]. However, to the author's knowledge, the TMCMC method has not been applied towards the Preisach model. Using the procedure discussed in the previous section, posterior PDFs for the Preisach model parameters can be determined.

To restrict the parameter space θ, two vectors θ_{min} and θ_{max} must be defined such that the following equation is true.

$$\theta(i)_{min} < \theta(i) < \theta_{max}(i), \quad 1 \le i \le d. \tag{6.7}$$

This parameter space determines where the initial samples can be generated and determines the feasible values that the parameters can take. As previously mentioned, the prior PDFs for the parameters are assumed to be uniform between the constraints, and the likelihood PDF is defined as the prediction error. This is assumed to be Gaussian with zero mean and unknown variance. The prediction error is defined as the difference between the predicted simulated system response and the experimental system response.

$$f(D|\theta) = \prod_{i=1}^{l} \frac{1}{\sigma_{acc}\sqrt{2\pi}} exp\left[\frac{-1}{2\sigma_{acc}^2}\left(\frac{x(t_i) - \hat{x}(t_i|\theta)}{S_{acc}(t_i)}\right)^2\right]. \tag{6.8}$$

In Eq. (6.8), σ_{acc} represents the variance of the prediction errors and S_{acc} represents the weighting function used to normalize the acceleration response of the hysteretic system. Lastly, the log-likelihood function is used as the fitness function for the prediction error in Eq. (6.9).

$$lnf(D|\theta) = -\frac{1}{2}N_t \ln(2\pi) - N_t \ln\sigma_{acc} - \frac{-1}{2\sigma_{acc}^2}\left(\frac{x(t_i) - \hat{x}(t_i|\theta)}{S_{acc}(t_i)}\right)^2. \tag{6.9}$$

Next, with this setup, the TMCMC can be performed with experimental loops and be fitted using the Preisach model. These results will be compared against the more traditional LSQ fitting for total error and run time.

Shown in Figure 6.2 is an example of the TMCMC on some of the aforementioned experimental data.
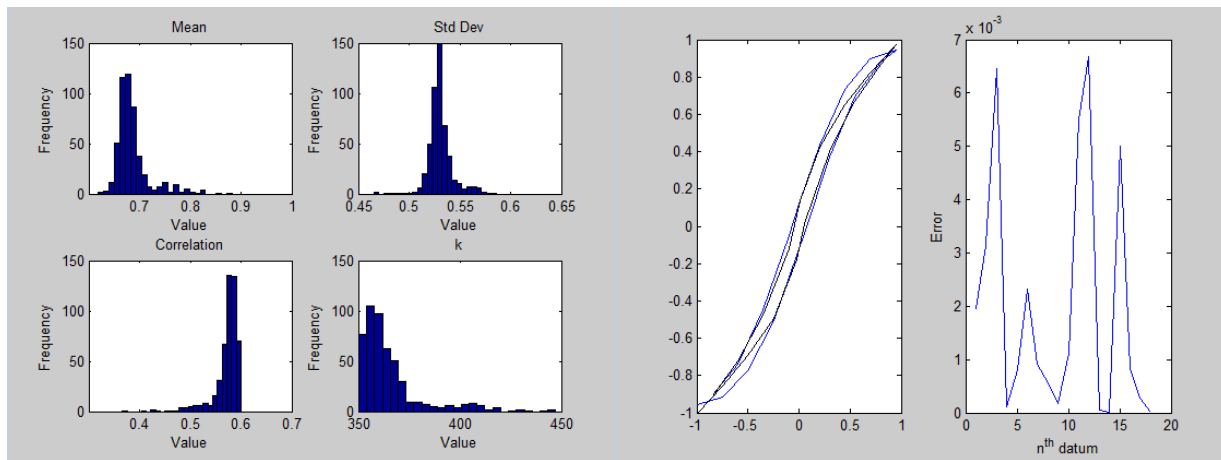
Figure 6.2: TMCMC Preisach model with Case 1; posterior PDF (left) and loop fit (right)

The parameters for this fitting are also outputted further in Table 6.1 (to compare against the LSQ method). They are assumed to be the peak in each of the PDFs. To further establish the feasibility of the TMCMC, Figure 6.3 is also produced, pertaining to the "square" hysteresis example.
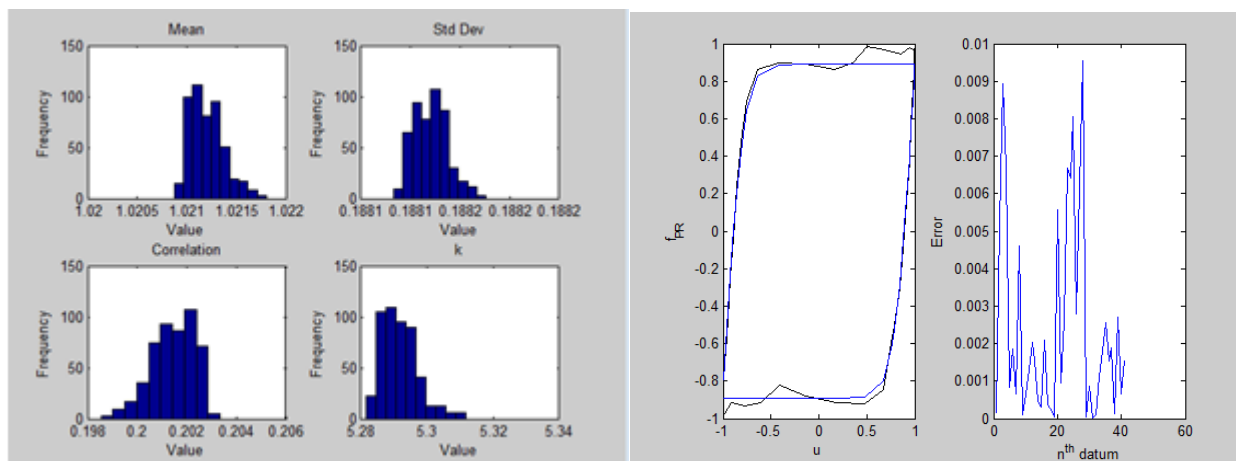
Figure 6.3: TMCMC Preisach model with Case 4; posterior PDF (left) and loop fit (right)

Now that the model has proven effectiveness, it can be compared against the LSQ method. In Table 6.1, these approaches are evaluated.

Case #	$|\mu|$	σ	ρ	k	Error	Error/point	Run Time (s)
1 LSQ	0.9988	0.5442	0.1783	426.875	0.0756	0.0042	39.86
1 TMCMC	0.7225	0.5448	0.5636	370.419	0.1174	0.0065	705.17
2 LSQ	0.3778	0.069	0.9977	0.9442	0.1409	0.0046	24.43
2 TMCMC	0.3792	0.0655	0.5992	0.8917	0.2154	0.0071	1338.62
3 LSQ	1.6321	0.2921	-0.933	94.7101	0.0684	0.0016	64.09
3 TMCMC	1.5683	0.2724	-0.856	96.9413	0.0988	0.0024	1302
4 LSQ	2.7694	1.6082	0.2458	125.392	0.0935	0.0022	54.07
4 TMCMC	2.7459	1.6352	0.2622	112.591	0.1134	0.0059	1950
5 LSQ	0.0804	0.1676	-0.67	1.3304	0.9681	0.0115	82
5 TMCMC	0.1207	0.1412	-0.591	1.0671	0.5094	0.0121	2385

Table 6.1: Comparison of LSQ and TMCMC methods for Preisach model

The fits for all of these comparisons are captured in Figure 6.4. Each of the subplots shows the comparison between the experimental data, LSQ, and TMCMC.
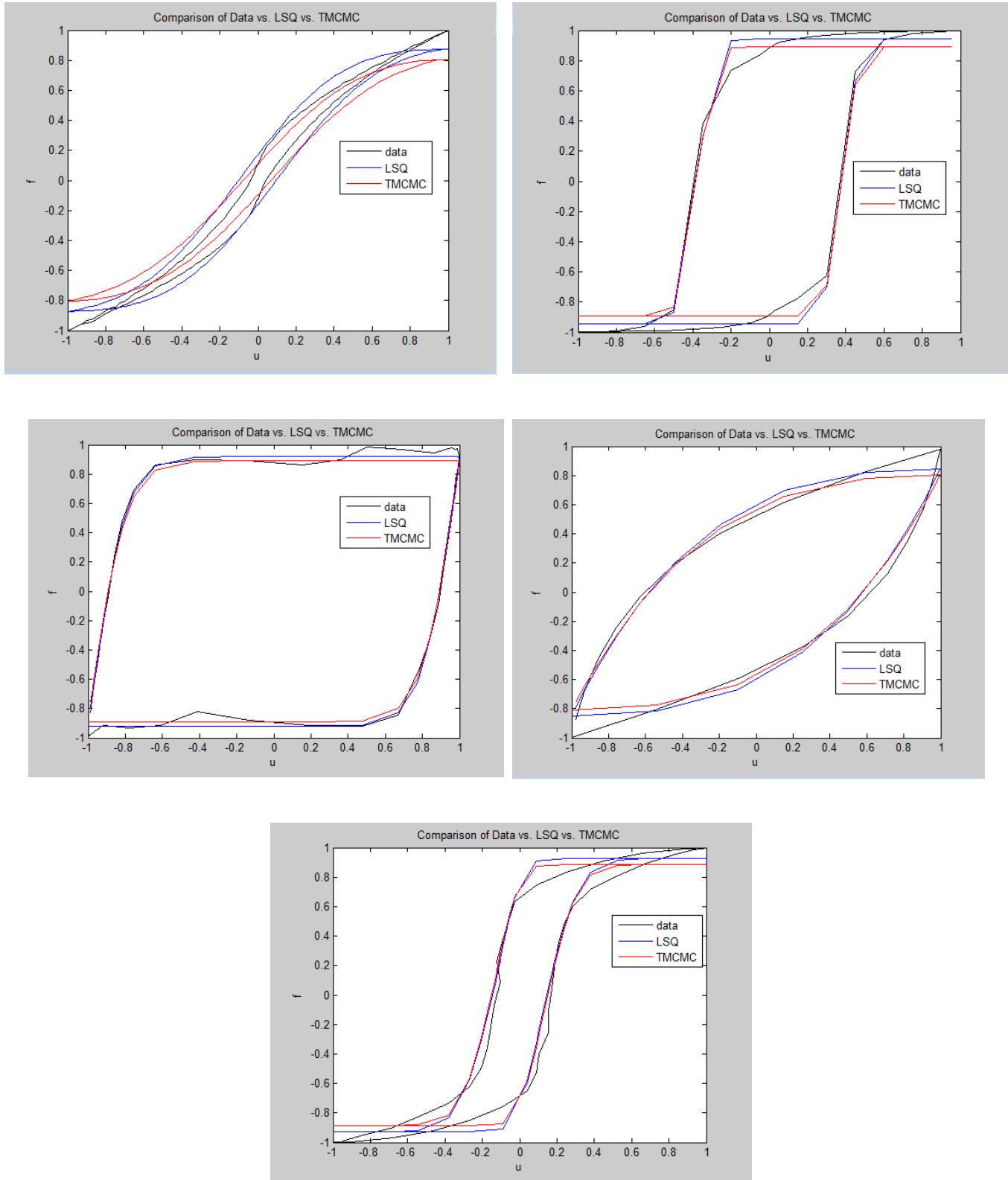
Figure 6.4: Hysteresis loops comparing LSQ and TMCMC vs. experimental data; Cases 1-5

As Figure 6.3 and Table 6.1 show, the TMCMC produces an essentially equally adequate fit for Preisach parameters as the LSQ method. However, the most evident downside from the data is the run time. While LSQ takes on the order of a minute or two, TMCMC takes upwards of 2000 seconds, or a little more than half an hour. Thus, it can be deduced that, in most circumstances, the LSQ method is preferred for expediency. That being said, there are scenarios where TMCMC could prove to be a versatile method. As the following section shows, the TMCMC method can be beneficial in producing a family of solutions via the posterior PDFs. Further, with the addition of white noise corruption, which can occur with real material samples, the TMCMC method can achieve levels of accuracy that the LSQ cannot.

6.4   Comparison of LSQ and TMCMC with a Theoretical Loop

An interesting phenomenon of the Preisach model is its versatility with parameter fitting. Indeed, due to interrelated and correlated variables, a loop can be approximated via two different methods very effectively, despite the methods generating different sets of parameters. An example is presented below. For this scenario, the theoretical loop to be compared against has the following parameters, presented in Table 6.2.

$|\mu|$	σ	ρ	k
0.6	0.75	0.3	2.67

Table 6.2: Theoretical Preisach model true parameters

Figure 6.5 and Table 6.3 show the result of the best fit for both the LSQ and TMCMC approaches.
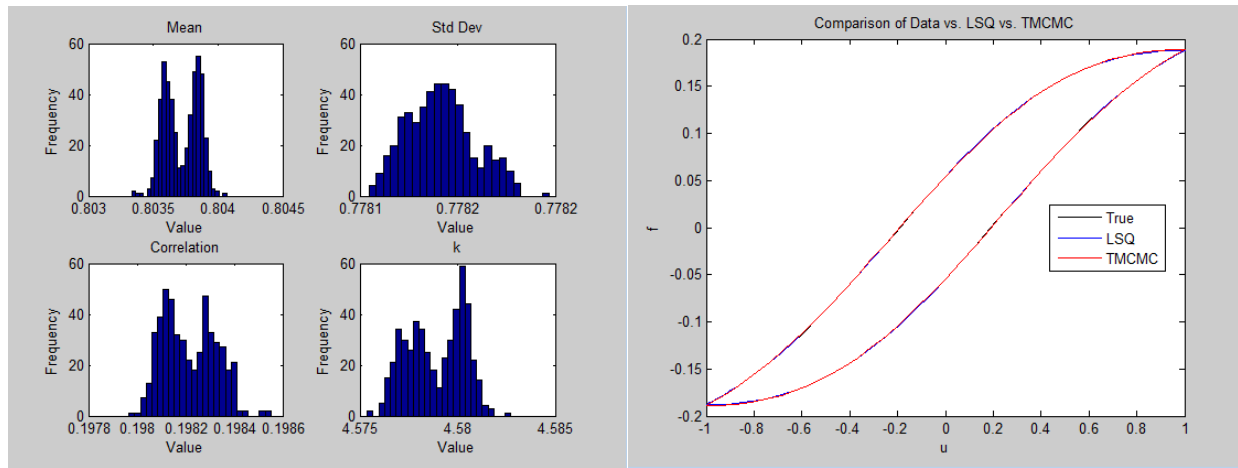
Figure 6.5: Theoretical hysteresis loop compared with LSQ and TMCMC approaches; posterior

PDF (left) and loop fits (right)

Parameters	$|\mu|$	σ	ρ	k	Err	Err/point	Run Time (s)
True	0.6	0.75	0.3	2.67	−	−	−
LSQ	0.858	0.785	0.172	5.275	$4.58E - 08$	$4.54E - 10$	27.05
TMCMC	0.803	0.778	0.198	4.580	$5.96E - 05$	$5.90E - 07$	1767.21

Table 6.3: True parameters compared with LSQ and TMCMC parameters

Thus, both methods adequately capture the hysteresis loop, even with different sets of
parameters. This demonstrates the flexibility of the Preisach model in capturing curves in
different manners.

6.5   Theoretical Loop Subjected to White Noise Compared to LSQ and TMCMC

Another useful application of the TMCMC approach regards the response of a hysteretic element corrupted by noise. To simulate this, the theoretical hysteresis loop in Section 6.4 is subjected to white noise excitation. The same approach for both methods is incorporated. The results are captured in Figure 6.6 and Table 6.4.
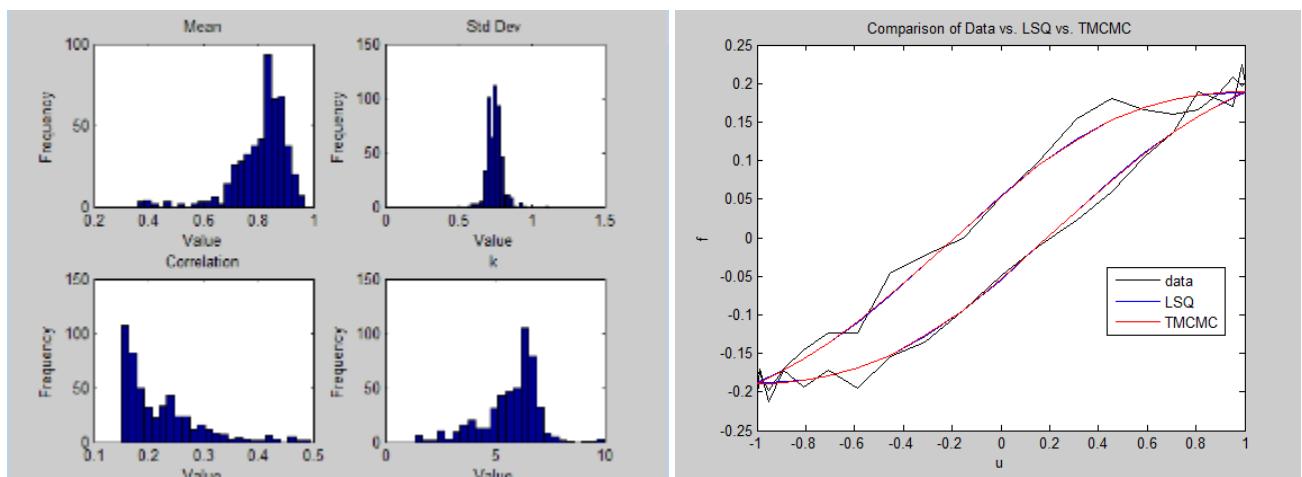
Figure 6.6: Theoretical Noisy Loop Compared with LSQ and TMCMC; posterior PDF (left) and loop fit (right)

Parameters	$|\mu|$	σ	ρ	k	Err	Err/point	Run Time (s)
True	0.6	0.75	0.3	2.67	—	—	—
LSQ	0.6698	0.6904	0.0593	2.8898	0.016	$3.9024E-4$	158
TMCMC	0.9104	0.8716	0.3503	7.7468	0.0133	$3.243E-4$	1993

Table 6.4: True parameters subjected to white noise compared with LSQ and TMCMC parameters

As it can be deduced from this example, the TMCMC approach can prove useful in situations with noisier loops. Indeed, even though the TMCMC approach still takes far longer, it minimizes the error more effectively (albeit marginally) than LSQ. Thus, with loops subjected to noise, the TMCMC approach can prove to be an effective approach to capture loops that are harder to model.

6.6   Loops Optimized via Combined TMCMC and LSQ

Much of the challenge in using any identification problem algorithm scheme lies in the choice of the searched parameter space. This is certainly a limiting factor in the applicability of the Bouc-Wen model; it is difficult to find the optimized parameter space in which to perform any LSQ approach. One of the advantages of the Preisach model is its ability to optimize over the wide bounds described in Table 3.2.

However, the LSQ for the Preisach model can reach a stalemate in a local minimum in the same manner as the Bouc-Wen model, albeit to a much lesser degree. To account for this, it is helpful to have a more refined search space and initial estimate. This is one of the benefits of the TMCMC method. Using TMCMC first on an experimental data set, the optimized parameters can be estimated within a much smaller margin of error via the peaks on the posterior Gaussian PDFs. After this, the LSQ algorithm can be performed with the initial estimate from the TMCMC method and a tighter margin for the parameter search space. Figure 6.7 affords a visual comparison of three loops approximating an experimental loop via the Preisach model: LSQ, TMCMC, and lastly TMCMC followed with LSQ. Table 6.6 shows the parameters for each of the solutions.
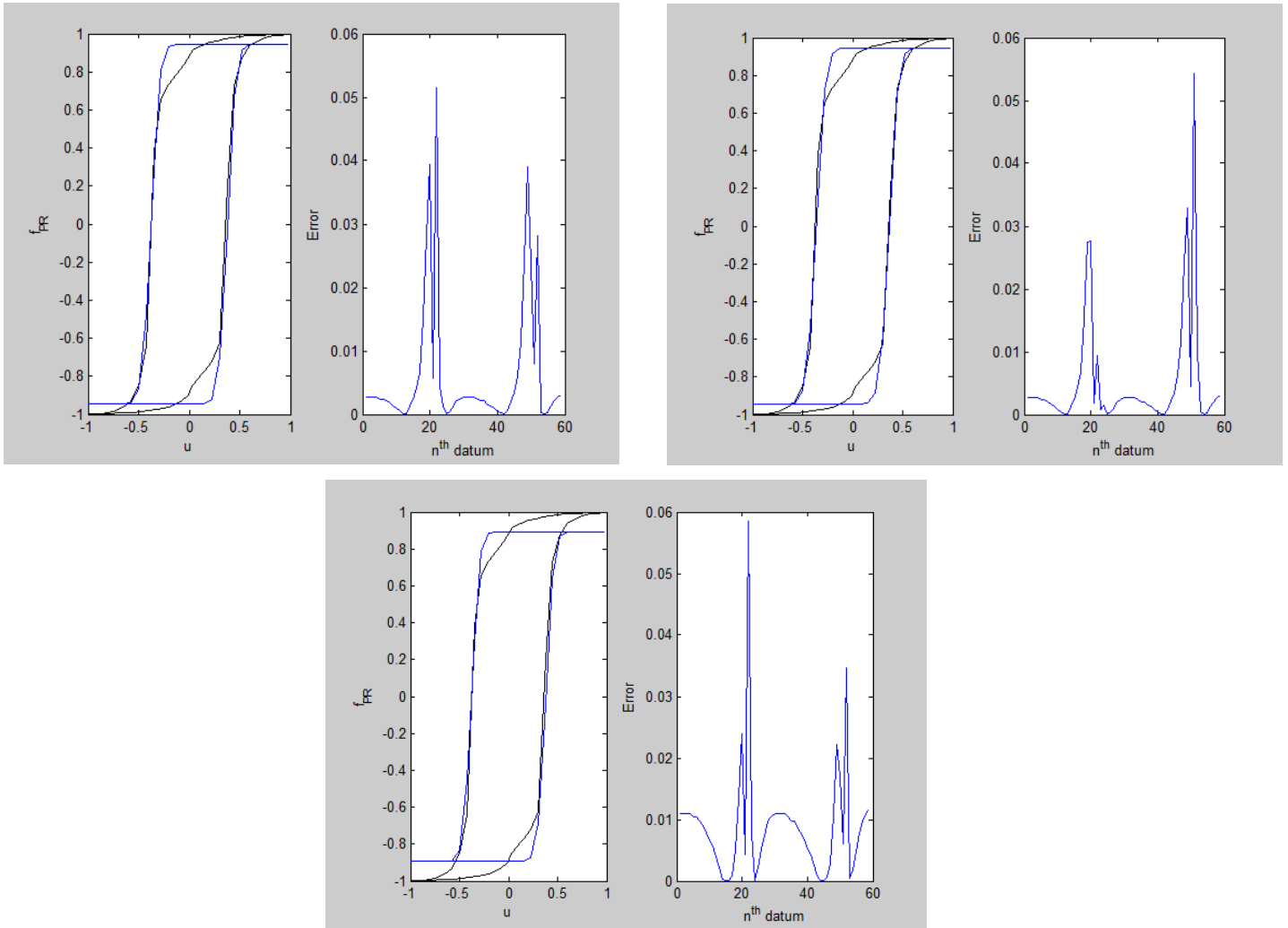
Figure 6.7: Preisach model with LSQ (top left), TMCMC (top right), and the combination of

both (bottom)

Scenario	$|\mu|$	σ	ρ	k	Error	Error/point
LSQ	0.3778	0.069	0.9977	0.9442	0.3668	0.006217
TMCMC	0.3792	0.0655	0.5992	0.8917	0.5109	0.008659
Combination	0.3778	0.069	0.9977	0.9442	0.3068	0.0052

Table 6.6: Preisach parameters comparing LSQ, TMCMC, and the combination of both

This example shows that the sequential combination of using TMCMC and LSQ with a more refined initial estimate and search space leads to the best results. Both figures and table show that the difference is rather small. However, if one wanted a very refined model and search space, using the combination of TMCMC and LSQ is the optimal method out of the ones presented in this work to lead to the minimal root mean square error.

This can be applied towards the hysteresis loop discussed in the previous section with the theoretical loop subjected to white noise. Using the same procedure as discussed above, the theoretical loop with the parameters outlined in Table 6.2 is subjected to white noise corruption and is subsequently analyzed via the three methods. Pertinent results are shown in Figure 6.8 and Table 6.7.

(a)

(b)

(c)

(d)
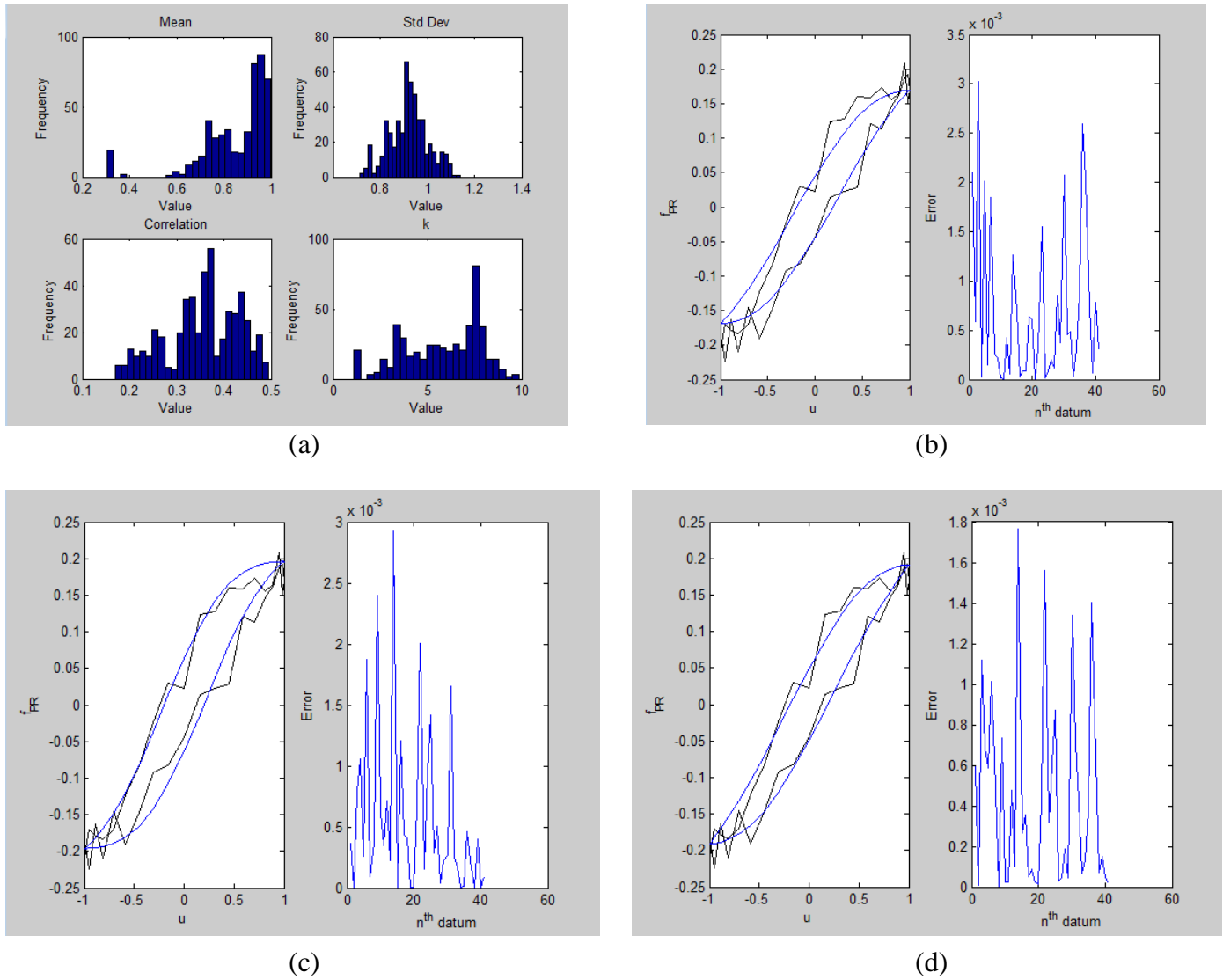
Figure 6.8: Preisach model posterior PDF (a), TMCMC fit (b), LSQ fit (c), and combined

TMCMC and LSQ fit (d)

Scenario	$|\mu|$	σ	ρ	k	Error	Error/point
LSQ	0.6698	0.6904	0.0593	2.8898	0.0239	0.000693
TMCMC	0.9643	0.9062	0.3490	7.6601	0.0284	0.000583
Combination	0.8743	0.8381	0.3058	6.4955	0.0182	0.000444

Table 6.7: Preisach parameters comparing LSQ, TMCMC, and the combination of both for

theoretical white noise loop

As Figure 6.8 and Table 6.7 show, the combination of the TMCMC method and the LSQ method minimizes the normalized error most effectively.

6.7   Summary

The TMCMC method has proven effective towards its application with the Preisach model. It approaches a similar degree of accuracy that the LSQ method does. Although the requisite computational time makes TMCMC less desirable than LSQ in simple cases, there are scenarios where the TMCMC method is preferred:

1) When the user wants more information on the family of solutions around the peaks on the posterior Gaussian PDFs (namely the distribution of data).

2) When white noise is introduced.

Further, a combination of using the TMCMC method first for a good approximate solution followed by the LSQ method with a very accurate initial estimate and tighter bounds proves to be the more accurate method of all examined in this study. If the user wants an extra degree of accuracy, the combination of TMCMC and LSQ is the superior method.

Chapter 7

Concluding Remarks

Many systems in a wide variety of engineering applications exhibit hysteretic behavior, ranging from aircraft wings to magnets. Thus, it is an important concern of engineers to be able to model hysteresis accurately for a more efficient design strategy. In this context, there were three main goals of this thesis. First, an algorithm has been developed that converts equivalent hysteresis loop approximations from the Bouc-Wen model to the Preisach model and vice versa. Second, the Preisach model and Bouc-Wen model have been evaluated and applied on a series of experimental data supplied by AFRL. Third, the TMCMC method has been applied in conjunction with the Preisach model and evaluated against other identification problem methods.

In *Chapter 1*, the hysteresis phenomenon has been defined and its main characteristics specified. Further, it has covered a brief history of the field and the need for effective modeling of hysteresis. It has been clarified that there are two major modeling techniques of hysteresis which relates to local and nonlocal memory. From the local memory models, the Bouc-Wen model has been developed. From the nonlocal memory models, Preisach formalism has been developed.

Chapter 2 has built upon this base laid by the previous chapter by discussing the mathematical theory behind the methods used throughout the rest of the thesis. Preisach formalism has been formally introduced with the mathematical construction behind concepts such as the hysteron, the Preisach half-plane, and the density function. The identification problem for the Preisach

model has been discussed, with Eq. (2.6) being proposed as the bivariate Gaussian distribution approximation for the density function by Spanos et al [18, 19, 20, 22]. The Bouc-Wen model has been discussed in depth with the mathematical background for the system of differential equations that define it. The architecture of ANNs has been addressed and how they might be applied towards the conversion of Bouc-Wen parameters to Preisach parameters. Finally, some consideration has been given to the nature of Monte Carlo simulation that serves as the groundwork for the more detailed discussion regarding TMCMC in *Chapter 6*.

This theory has been applied in *Chapter 3* towards converting Bouc-Wen parameters into Preisach parameters through a couple of methods. First, the conversion has been accomplished via the LSQ method. Then, the alternative approach of incorporating an ANN has been proposed. The ANN has been built and trained with a library of randomized hysteresis loops within bounds being minimized with LSQ. Upon assessing the performance, it has been determined that both methods are accurate, but the ANN encounters more difficulty with more atypical loop shapes. The Bouc-Wen model is inherently not as flexible of a model (in this form) as the Preisach model. Thus, the ANN is useful for its near instantaneous computational speed, but is limited by the Bouc-Wen model's inflexibility with atypical loop shapes. Although this thesis advocates for the Preisach model being more flexible in nature than the Bouc-Wen model, *Chapter 3* also demonstrates the reverse direction of drawing Bouc-Wen parameters out of Preisach parameters, should the need for the researcher arise.

Chapter 4 has dealt with revisiting the parameters of both models. Since both models have several parameters to coordinate between, it is critical to have a competent initial estimate for the

parameters. Otherwise, the minimization process can become trapped in a local minimum. To make this sophisticated initial estimate, each parameter of each model has been investigated individually to evaluate its effect on the overall size and shape of the hysteresis loop. For each model, examples have proven the validity of the established guidelines for the determining of initial parameters.

Building upon this knowledge, *Chapter 5* has applied both the Preisach model and the Bouc-Wen model towards experimental data supplied by AFRL. Both methods have been evaluated via normalized error towards these loops. It has been shown that the Preisach model generally proves superior to the Bouc-Wen model in minimizing a wide variety of hysteresis loops. However, in practice, the Bouc-Wen model is not without merit, as it can be applied successfully towards materials with local memory. Further, more advanced variants of the Bouc-Wen model might perform better when compared to the Preisach model.

Finally, *Chapter 6* has been concerned with the application of TMCMC in conjunction with the Preisach model. The TMCMC method has proven quite effective in minimizing the supplied AFRL data, as well as theoretical loops. It has been shown that the LSQ method performs slightly better than the TMCMC method but that both are adequate. However, the TMCMC method proves to minimize error better when white noise is introduced with a theoretical loop. Thus, TMCMC is better at minimizing error than LSQ with "noisier" loops. It is then proposed that a combination of both TMCMC and LSQ is superior to either one separately, as using TMCMC first gives an excellent initial estimate with the peak of the posterior Gaussian PDF that can minimize error further with a more refined parameter search space for LSQ.

Further work could perhaps include investigating hysteresis models with multiple degrees of freedom. With this more complex approach, algorithms can be developed that determine the Preisach and Bouc-Wen models with more degrees of freedom. Conversion between the two models can be accomplished, and their performance toward experimental data can be analyzed. Further, instead of using the Bouc-Wen model, the more complex BWBN model (or other variations on the Bouc-Wen model) can be analyzed and compared against the Preisach model. Next, a formal sensitivity analysis can be performed to determine how each parameter for each model affects the loop. The relationships between the Bouc-Wen variables can be evaluated more closely via a correlation matrix (which can be accomplished via TMCMC data) to deduce redundant variables, as some research by Ma et al. suggests [74]. Finally, there can be further study into the modeling experimental minor loops for materials with nonlocal memories with the Preisach model

List of References

[1]   Brokate, M., and Sprekels, J. (1996). *Hysteresis and Phase Transitions*, Springer.

[2]   Lagoudas, D. C., Mayes, J. J., and Khan, M. M. "Parametric study and experimental correlation of an SMA based damping and passive vibration isolation device." *ASME International Mechanical Engineering Congress & Exposition*, New Orleans, Louisiana, 13-26.

[3]   Ewing, J. A., 1885, "Experimental Researches in Magnetism," Phil. Trans. R. Soc. London, **176**, pp. 523-640.

[4]   Morris, K. A. "What is Hysteresis?" *American Society of Mechanical Engineers* 64 (2011): Web.

[5]   Rayleigh, J. W. S. B. (1887). "On the behavior of iron and steel under the operation of feeble magnetic force." *The Philosophical Magazine*, 5(XXIII), 225-245.

[6]   Duhem, P. (1897). "Die dauernden Anderungen und die Thermodynamik I: Die Dauernden Angerungen der Systeme, welche von einer einzigen normalen Veranderlichen abhangen" [The Constant Changes and Thermodynamics I: The Continuing Considerations of Systems Dependent on a Single Normal Change]. *Zeitschrift fur Physik und Chimie*, 22, 543-589.

[7]   Preisach, F. (1935). "Uber die magnetische Nachwirkung" [On the magnetic after-effects]. *Zeitschrift fur Physik*, 94, 227-302.

[8]   Mises (von), R. (1913). "Mechanik der festoon Korper in plastisch-deformablen Zustand" [Mechanics of solid bodies in the plastically-deformable state]. *Gottinger Nachr. Akad. Wiss., Math. Phys.*, KI, 582-592.

[9]   Prandtl, L. "Spannungverteilung in plastischen Korpern" [Stress distribution in plastic bodies]. *1st International Congress on Applied Mechanics*, Delft, The Netherlands, 43-54.

[10]   Ishlinskii, A. Y. (1954). "General theory of plasticity with linear strain-hardening." *Ukrain. Matem. Zhurnal*, 6, 314-328.

[11]   Hill, R. (1948). "A variational principle of maximum plastic work in classical plasticity." *The Quarterly Journal of Mechanics and Applied Mathematics*, 1, 18-28.

[12]   Prager, W. (235). "Recent developments in the mathematical theory of plasticity." *Journal of Applied Physics*, 20, 235-241.

[13]   Bouc, R. "Forced vibrations of a mechanical system with hysteresis." *Proceedings of the 4th conference on nonlinear oscillations*, Prague.

[14]   Krasnoselskii, M. A., and Pokrovskii, A. V. (1983). *Systems with Hysteresis*, Springer-Verlag.

[15]   Mayergoyz, I. (2003). *Mathematical models of Hysteresis and Their Applications*, Elsevier.

[16]   Ismail, Mohammed, Fayçal Ikhouane, and José Rodellar. "The Hysteresis Bouc-Wen Model, a Survey." *Archives of Computational Methods in Engineering* 16.2 (2009): 161-88. Web.

[17]   Kontsos, Antonios. *Deterministic and Random Analysis of Systems with Hysteresis using the Preisach Formalism.* Dissertation, Rice University, 2004.

[18]   Ktena, A., Fotiadis, D. I., Spanos, P. D., Berger, A., and Massalas, C. V., 2002, "Identification of 1D and 2D Preisach Models for Ferromagnets and Shape Memory Alloys," *Int. J. Eng. Sci.,* **40**, pp. 2235-2247.

[19]   Ktena, A., Fotiadis, D. I., Spanos, P. D., and Massalas, C. V., 2001, "A Preisach Model Identification Procedure and Simulation of Hysteresis in Ferromagnets and Shape-Memory Aloys," *Physica B*, **306**, pp. 84-90.

[20]   Spanos, P. D., A. Kontsos, and P. Cacciola. "Steady-State Dynamic Response of Preisach Hysteretic Systems." *Journal of Vibration and Acoustics* 128.2 (2006): 244. Web.

[21]   Spanos, P.D., Cacciola, P., and Muscolino, G., 2004, "Stochastic Averaging of Preisach Hysteretic Systems," *J. Eng. Mech.,* **130**(11), pp. 1257-1267.

[22]   Spanos, P.D., Cacciola, P., and Redhorse, J., 2004, "Random Vibration of SMA Systems via Preisach Formalism," *Nonlinear Dyn.*, **36**(2-4), pp. 405-419.

[23]   Ni, Y. Q., Ko, J. M., and Wong, C. W. (1999). "Nonparametric identification of nonlinear hysteretic systems." *Journal of Engineering Mechanics*, 125(2), 206-215

[24]   Ikhouane, F., Hurtado, J. E., and Rodellar, J., "Variation of the hysteresis loop with the Bouc-Wen model parameters," *Nonlinear Dyn*. 48(4) (2007) 361-380.

[25]   Laudani, A., Fulginei, F. R., Salvini, A., "Bouc-Wen hysteresis model identification by the metric-topological evolutionary optimization," *IEEE Trans. Magn*. 50(2) (2014) 621-624.

[26] Giuclea, M., Sireteanu, T., Mitu, A. M., "Use of genetic algorithms for fitting the Bouc-Wen model to experimental hysteretic curves," *Rev. Roum. Sci. Techn.-Mec. Appl. Tome* 54 (2009) 3-10.

[27] Ye, M., Wang, X., "Parameter estimation of the Bouc-Wen hysteresis model using particle swarm optimization," *Smart Mater. Struct.* 16(2007) 2341-2349.

[28] Zaman, Mohammad Asif, and Urmita Sikder. "Bouc–Wen hysteresis model identification using Modified Firefly Algorithm." *Journal of Magnetism and Magnetic Materials* 395 (2015): 229-33. Web.

[29] Gerald, C. F., Wheatley, P. O., *Applied Numerical Analysis*, Seventh Edition, Pearson, London, U. K.

[30] R. Hecht-Nielsen, *Neurocomputing*, Addison-Wesley, Reading, Mass, USA, 1989.

[31] Xie, S.l., Y.H. Zhang, C.h. Chen, and X.N. Zhang. "Identification of nonlinear hysteretic systems by artificial neural network." *Mechanical Systems and Signal Processing* 34.1-2 (2013): 76-87. Web.

[32] S.F. Masri, A.G. Chassiakos, T.K. Caughey, "Structure-unknown non-linear dynamic systems: identification through neural networks," *Smart Mater. Struct.* 1 (1992) 45–46.

[33] A.W. Smyth, S.F. Masri, E.B. Kosmatopoulos, A.G. Chassiakos, T.K. Caughey, "Development of adaptive modeling techniques for non-linear hysteretic systems," *Int. J. Non Linear Mech.* 37 (2002) 1435–1451.

[34]   Trapanese, Marco. "Identification of parameters of dynamic Preisach model by neural networks." *Journal of Applied Physics* 103.7 (2008): n. pag. Web.

[35]   Zakerzadeh, Mohammad Reza, Mohsen Firouzi, Hassan Sayyaadi, and Saeed Bagheri Shouraki. "Hysteresis Nonlinearity Identification Using New Preisach Model-Based Artificial Neural Network Approach." *Journal of Applied Mathematics* 2011 (2011): n. pag. Web.

[36]   Farrokh, Mojtaba, and Abdolreza Joghataie. "Adaptive Modeling of Highly Nonlinear Hysteresis Using Preisach Neural Networks." *Journal of Engineering Mechanics* 140.4 (2014): 06014002. Web.

[37]   Trapanese, Marco, Maurizio Cirrincione, , Rosario Miceli, and Giuseppe Ricco Galluzzo. "Preisach's function identification by neural network." *IEEE Transactions on Magnetics* 38.5 (2002): 2421-423. Web.

[38]   Politis, N. P. (2002). "An approach for efficient analysis of drill-string random vibrations," Master of Science, Rice University.

[39]   Spanos, P., T-D. (1976). "Linearization Techniques for Nonlinear Dynamical Systems," report EERL 76-4., California Institute of Technology.

[40]   Fishman, G. S. (1996). *Monte Carlo – Concepts, algorithms, and applications*, Springer.

[41]   Kalos, Malvin H., and Paula A. Whitlock. *Monte Carlo methods.* N.p.: John Wiley & Sons, Ltd., 1986. Print.

[42]   Liu, J. S. (2001). *Monte Carlo strategies in scientific computing*, Springer.

[43]   Rubinstein, R. Y. (1981). *Simulation and the Monte Carlo method*, John Wiley & Sons.

[44]   Tsavachidis, S. (2000). "Deterministic and Random analysis of nonlinear systems with Biot hysteretic damping," Master of Science, Rice University.

[45]   Bretscher, Otto (1995). *Linear Algebra With Applications* (3rd ed.). Upper Saddle River, NJ: Prentice Hall.

[46]   Stigler, Stephen M. (1981). "Gauss and the Invention of Least Squares." *Ann. Stat*. **9** (3): 465–474.

[47]   M. Ye, X. Wang, "Parameter identification of hysteresis model with improved particle swarm optimization," Chinese Control and Decision Conference, 2009. CCDC'09, IEEE, Guilin, China, 2009, pp. 415-419.

[48]   Solomon, Ovidiu. "Some Typical Shapes of Hysteretic Loops Using the Bouc-Wen Model." *Journal of Information Systems and Operations Management* 7.1 (2013): 73-82. Web.

[49]   Charalampakis, Aristotelis E. "Parameters of Bouc-Wen Hysteretic Model Revisited." *9th HSTAM International Congress on Mechanics, Limassol, Cyprus 12-14 July* (2010): n. pag. Web.

[50]   Spanos, P., "Linearization techniques for nonlinear dynamical systems', California Institute of Technology, Report EERL 76-4, 1976.

[51]   Iwan, W.D. and Spanos, P., 'Response envelope statistics for nonlinear oscillators with random excitation', *ASME Journal of Applied Mechanics* **45**, 1978, 170-178.

[52]   T. T. Baber, Y. K. Wen, "Random vibration hysteretic, degrading systems", Journal of the Engineering Mechanics Division, 1981 107(6) 1069-87.

[53]   T. T. Baber, Y. K. Wen, "Stochastic response of multistory yielding frames*", Earthquake Engineering & Structural Dynamics*, 1982 10(3) 403-16.

[54]   T. T. Baber, "Nonzero mean random vibration of hysteretic systems", *Journal of Engineering Mechanics*, 1984 110(7) 1036-49.

[55]   T. T. Baber, M.N. Noori, "Random vibration of degrading, pinching systems", *Journal of Engineering Mechanics,* 1985, DOI: http://dx.doi.org/10.1061/(ASCE)0733-9399(1985)111:8(1010).

[56]   T. T. Baber, "Modal analysis for random vibration of hysteretic frames", *Earthquake Engineering & Structural Dynamics,* 1986 14(6) 841-59.

[57]   T. T. Baber, "Nonzero mean random vibration of hysteretic frames", *Computers & Structures*, 1986 23(2) 265-77.

[58]   Beck, J. L. and Katafygiotis, L.S. (1998). "Updating models and their uncertainties – Bayesian statistical framework." *Journal of Engineering Mechanics*. **124**(4), 455-461.

[59]   Katafygiotis, L. S., Papadimitriou, C., and Lam, H. F. (1998). "A probabilistic approach to structural model updating." *Soil Dynamics and Earthquake Engineering*. **17** 495-507.

[60]   Vanik, M.W., Beck, J.L., and Au, S.K. (2000). "A Bayesian probabilistic approach to structural health monitoring." *Journal of Engineering Mechanics*. **126**, 738-745.

[61]   Kerschen, G., Golvinal, J.C., and Hemkez, F.M. (2003). "Bayesian model screening for the identification of nonlinear mechanical structures." *Journal of Vibration and Acoustics*. **125**, 389-397.

[62]   Yuen, K.V., Au, S.K., and Beck, J.L. (2004). "Two-stage structural health monitoring approach for Phase I benchmark studies." *Journal of Engineering Mechanics*, **130**, 16-33.

[63]   Ching, J. and Beck, J.L. (2004). "Bayesian analysis of the Phase II IASC-ASCE Structural Health Monitoring Experimental Benchmark Data." *Journal of Engineering Mechanics*, **130**(10), 1233-1244.

[64]   Metropolis, N., Rosenbluth, A.W., Rosenbluth, M.N., Teller, A.H., Teller, E. 1953. "Equation of state calculations by fast computing machines." *Journal of Chemical Physics*, 21, 1087-1092.

[65]   Hastings, W.K. 1970. "Monte Carlo sampling methods using Markov chains and their applications." *Biometrika* 57, 97-109.

[66]   Ching, Jianye, and Jiun-Shiang Wang. "Application of the transitional Markov chain Monte Carlo algorithm to probabilistic site characterization." *Engineering Geology* 203 (2016): 151-67. Web.

[67]   Gilks, Walter R., Sylvia Richardson, and D. J. Spiegelhalter. *Markov chain Monte Carlo in practice*. Boca Raton etc.: Chapman and Hall, 1998. Print.

[68]   Ching, J., Chen, Y.-C. 2007. "Transitional Markov chain Monte Carlo method for Bayesian model updating, model class selection and model averaging." *ASCE Journal of Engineering Mechanics*, 133(7) 816-832.

[69]   Beck, J.L., Au, S.K. 2002. "Bayesian updating of structural models and reliability using Markov chain Monte Carlo simulation." *ASCE Journal of Engineering Mechanics*, 128(4), 380-391.

[70]   Neal, R.M. 2001. "Annealed importance sampling." *Statistics and Computing*, 11, 125-139.

[71]   Zhao, Y., Noori, M., Altabey, W.A. 2017. "A Comparison of Three Different Methods for the Identification of Hysteretically Degrading Structures Using BWBN Model." Manuscript submitted for publication.

[72]   Muto, M., Beck, J.L. 2008. "Bayesian Updating and Model Class Selection for Hysteretic Structural Models Using Stochastic Simulation." *Journal of Vibration and Control*, **14(1-2)**: 7 – 34.

[73]   Ortiz GA et al. Identification of Bouc–Wen type models using the Transitional Markov Chain Monte Carlo method. *Computers and Structures* (2014), http://dx.doi.org/10.1016/j.compstruc.2014.10.012.

[74]   Ma, F., Zhang, H., Bockstedte, A., Foliente, G.C., Paevere P., "Parameter analysis of the differential model of hysteresis." *Journal of Applied Mechanics* 2004. 71(3):342-9.